

American University in Cairo

AUC Knowledge Fountain

Theses and Dissertations

Student Research

2-1-2016

Noncoherent MIMO codes for low-medium SNRs, and layered MIMO space-time coding for coherent and noncoherent receivers

Mohamed Ali ElMossallamy

Follow this and additional works at: <https://fount.aucegypt.edu/etds>

Recommended Citation

APA Citation

ElMossallamy, M. (2016). *Noncoherent MIMO codes for low-medium SNRs, and layered MIMO space-time coding for coherent and noncoherent receivers* [Master's Thesis, the American University in Cairo]. AUC Knowledge Fountain.

<https://fount.aucegypt.edu/etds/364>

MLA Citation

ElMossallamy, Mohamed Ali. *Noncoherent MIMO codes for low-medium SNRs, and layered MIMO space-time coding for coherent and noncoherent receivers*. 2016. American University in Cairo, Master's Thesis. *AUC Knowledge Fountain*.

<https://fount.aucegypt.edu/etds/364>

This Master's Thesis is brought to you for free and open access by the Student Research at AUC Knowledge Fountain. It has been accepted for inclusion in Theses and Dissertations by an authorized administrator of AUC Knowledge Fountain. For more information, please contact thesisadmin@aucegypt.edu.

THE AMERICAN UNIVERSITY IN CAIRO

MASTER THESIS

**Noncoherent MIMO Codes for Low-Medium
SNRs, and Layered MIMO Space-Time
Coding for Coherent and Noncoherent
Receivers**

Author:

Mohamed Ali

ELMOSSALLAMY

Supervisor:

Dr. Karim SEDDIK

A thesis submitted in partial fulfillment of the requirements

for the degree of Master of Science

in the

Department of

Electronics and Communications Engineering

January 21, 2017

Abstract

Wireless communication systems rely on training the receiver to learn the channel state information (CSI) to communicate information effectively. In these coherent wireless communication systems, pilot signals known to the receiver are sent periodically to help the receiver learn CSI which is needed for effective detection. However, mobile wireless standards are constantly aiming to increase supported velocities and data rates. As the velocity of the receiver increase, the channel changes rapidly, and more frequent training is required, which compromise efficient communication of information. Moreover, multiple-antenna techniques are usually required nowadays to increase supported data rates, which increases the number of channel parameters that have to be estimated and thus requires longer training periods. This lead to significant research activity in wireless communication systems that do not require channel knowledge at the receiver for detection, and thus eliminate the need for training altogether. Those systems are called non-coherent.

In the first part of thesis, we propose an new approach to construct space-time codes for the multiple-input multiple-output (MIMO) noncoherent channel. Unlike designs which fixed the number of transmit antennas active at any signaling interval, in our designs we let the number of the active transmit antennas vary over constellation points. We use numerical simulations to evaluate the performance of our proposed designs. At low-to-moderate SNRs, simulations results suggest that our codes could provide significant performance gains over codes designed using direct numerical optimization and exponential mappings where the number of transmit antennas is fixed, especially at higher constellation cardinalities.

In the second part, we consider layered space-time signaling over the multiple input multiple output multicast channel. In our proposed scheme, information is encoded in two layers; a low-resolution layer and a high-resolution layer, and there are two classes of receivers; noncoherent receivers that do not have access to accurate CSI and are only able to decode the information in the low-resolution layer, and coherent receivers that have access to accurate CSI, and thus able to decode both the low-resolution and incremental high-resolution information. Low-resolution information is encoded using Grassmannian MIMO codes, while high-resolution information is encoded in the indices of the transmitter antennas active during the signaling interval using a scheme called *generalized space shift keying* (GSSK). The proposed HR layer is completely transparent to the LR layer. Moreover, we propose a computationally efficient two-step decoder. Simulation results suggest that the error performance of the proposed HR layer could be superior to existing schemes that uses conventional space-time codes synthesized from APM symbols and space-time codes designed by direct numerical optimization on the unitary group.

Acknowledgements

All praise to Allah, the most merciful and the most gracious.

I would like to express my deepest gratitude to my thesis advisor Dr. Karim Seddik. Words can not express how grateful I am for his patience, continuing support and sincere interest in my development. I am forever indebted to him for the knowledge he taught me and the support he gave me during my studies.

I also would like to thank Dr. Ayman Elezabi for his support during my time at the university. He is a great professor to whom I owe much of my understanding of Stochastic Processes and Communications Theory.

Finally, I am deeply indebted to all the professors who taught me courses during my studies at the university. In addition to Dr. Karim Seddik and Dr. Ayman Elezabi, I would like to thank Dr. Yasser Gadallah, Dr. Ahmed Abou-Auf and Dr. Mohamed Swillam for the knowledge they shared with me.

Contents

Abstract	iii
Acknowledgements	v
1 Introduction	1
1.1 Motivation	1
1.2 The Wireless Channel	2
1.3 Multiple Antenna Wireless Systems	4
1.4 Space-Time Coding	7
1.5 System Model	10
1.6 Literature Review	12
1.6.1 Noncoherent MIMO Codes	12
1.6.2 Coherent Codes	15
Design Criteria	16
1.7 Thesis Outline and Contributions	17
2 Non-coherent Grassmanian MIMO Codes for Low-to-Moderate SNRs	21
2.1 Introduction	22
2.2 Preliminaries and System Model	24
2.2.1 The Grassmann Manifold	24
2.2.2 Chordal Frobenius Distance	24
2.2.3 System Model	25
2.3 Code Construction and Decoding	26
2.3.1 Initial Constellation Design	28

2.3.2	Augmented Constellation	30
2.3.3	Decoder	31
2.4	Simulation Results	32
3	Multiresolution Multicasting using Grassmannian MIMO codes and Space Shift Keying	37
3.1	Brief Overview of Spatial Modulation	38
3.2	System Model	40
3.3	Code Structure	42
3.3.1	LR Layer (Non-coherent) Code Construction	42
3.3.2	HR Layer (coherent) Code Construction	43
3.4	Detectors	47
3.4.1	The Optimal Non-coherent Detector	47
3.4.2	Optimal (Joint) One Step Coherent Detector	48
3.4.3	Two Step Suboptimal Coherent Detector	49
3.5	Simulation Results	49
4	Conclusions and Future Work	55
4.1	Conclusions	55
4.2	Future Work	56
A	Conjugate Gradient on The Grassmann Manifold	57
	Bibliography	61

List of Figures

1.1	Multiple Antenna Communication System	4
1.2	Generic MIMO Communication System	7
2.1	Performance of the augmented constellation against the ones in [15] (Direct, $M = 1$ and $M = 2$) and [22] (Exp.). For the Exp. constellation, s_1 and s_2 are drawn from 4-QAM const., where as s_3 and s_4 are drawn from BPSK const.	33
2.2	Performance of the augmented constellation against the ones in [15] (Direct, $M = 1$ and $M = 2$) and [22] (Exp.). For the Exp. constellation, s_1 , s_2 and s_3 are drawn from 4-QAM const., where as s_4 is drawn from BPSK const.	34
2.3	Performance of the augmented constellation against the ones in [15] (Direct, $M = 1$ and $M = 2$) and [22] (Exp.). For the Exp. constellation, s_1 , s_2 , s_3 and s_4 are drawn from 4-QAM const.	35
2.4	Performance of the augmented constellation against the ones in [15] (Direct, $M = 1$ and $M = 2$) and [22] (Exp.). For the Exp. constellation, s_2 , s_3 and s_4 are drawn from 4-QAM const., where as s_1 is drawn from 8-QAM const.	35

2.5	Performance of the augmented constellation against the ones in [15] (Direct, $M = 1$ and $M = 2$) and [22] (Exp.). For the Exp. constellation, s_1 , s_2 and s_3 are drawn from 8-QAM const., where as s_1 is drawn from BPSK const.	36
3.1	Illustration of the basic concept of Spatial Modulation .	38
3.2	BER performance of GSSK versus V-BLAST, and SM, for = 3 blts/s/Hz transmission ($N = 4$).	39
3.3	The MIMO Multicast System Model	41
3.4	Performance of the noncoherent detector. (256 point LR constellation constructed on $\mathbb{G}_{4,2}$ using the direct method)	50
3.5	Performance of the 2-step coherent detector. (256 point LR constellation constructed on $\mathbb{G}_{4,2}$ using the direct method and 4 point HR spatial constellation.)	50
3.6	Performance of the 1-step coherent detector. (256 point LR constellation constructed on $\mathbb{G}_{4,2}$ using the direct method and 4 point HR spatial constellation.)	51
3.7	Performance of the noncoherent detector. (2 point LR constellation constructed on $\mathbb{G}_{4,2}$).	52
3.8	Performance of the 2-step coherent detector. (2 point LR constellation constructed on $\mathbb{G}_{4,2}$ and 4 point HR spatial constellation.)	52
3.9	Comparison with the unitary code in [21] (2 point LR constellation constructed on $\mathbb{G}_{4,2}$ and 4 point HR constellations.)	53

List of Abbreviations

APM	Amplitude Phase Modulation
AWGN	Additive White Gaussian Noise
BER	Bit Error Rate
BLAST	Bell Laboratories Layered Space Time
BPSK	Binary Phase Shift Keying
CSI	Channel State Information
GSSK	Generalized Space Shift Keying
IAS	Inter-ANetna Synchronization
ICI	Inter-Channel Interference
iid	independent and identically distributed
MAP	Maximum A Posteriori
MIMO	Multiple-Input Multiple-Output
ML	Maximum Likelihood
OSTBC	Orthogonal Space Time Block Code
PDF	Probability Distribution Function
PEP	Pairwise Error Probability
PSK	Phase Shift Keying
QAM	Quadrature Amplitude Modulation
QPSK	Quadrature Phase Shift Keying
RF	Radio Frequency
SM	Spatial Modulation
SNR	Signal to Noise Ratio
SSK	Space Shift Keying

STBC **S**pace **T**ime **B**lock **C**ode

V-BLAST **V**ertical-**B**ell **L**aboratories **L**ayered **S**pace **T**ime

List of Symbols

x	the scalar x
$ x $	the absolute value of a scalar
x^*	the complex conjugate of a scalar
\mathbf{x}	the vector \mathbf{x}
\mathbf{x}^*	the complex conjugate of a vector
\mathbf{x}^T	the transpose of a vector
\mathbf{x}^\dagger	the Hermitian (conjugate transpose) of a vector
$\ \mathbf{x}\ $	the norm of a vector
\mathbf{X}	the matrix \mathbf{X}
\mathbf{X}^T	the transpose of a matrix
\mathbf{X}^\dagger	the Hermitian (conjugate transpose) of a matrix
$\ \mathbf{X}\ _F$	the Frobenius norm of a matrix
\triangleq	defined as equal to
$\exp(x)$	exponential of x (i.e. e^x)
$\binom{n}{k}$	the binomial coefficient (i.e. n choose k)
$P(A)$	the probability of an event A
$p_Y(y)$	the pdf of a random variable Y
$\log(x)$	the natural logarithm (i.e. base e)
$\log_a(x)$	the logarithm with base a
$\arg \max_x f(x)$	a value of x that maximizes the function $f(x)$
$\arg \min_x f(x)$	a value of x that minimizes the function $f(x)$
$X \sim p_X(x)$	the random variable X has PDF $p_X(x)$
\mathbf{I}_N	the $N \times N$ identity matrix

$\mathcal{N}\left(m, \frac{\sigma^2}{2}\right)$	the Gaussian distribution of a random variable, with mean m and variance $\frac{\sigma^2}{2}$
$\mathcal{CN}(m, \sigma^2)$	the complex Gaussian distribution of a random variable, having independent Gaussian distributed real and imaginary parts (i.e. $\text{real} \sim \mathcal{N}\left(m, \frac{\sigma^2}{2}\right)$, $\text{imaginary} \sim \mathcal{N}\left(m, \frac{\sigma^2}{2}\right)$)
ρ	denotes the average SNR at each receive antenna

Chapter 1

Introduction

1.1 Motivation

It is vital to design *multiple input multiple output* (MIMO) transceivers that are able to cope with various degrees of channel conditions and knowledge of *channel state information* (CSI) at the receiver. It is known that MIMO systems can achieve high gains over conventional *single input single output* (SISO) systems when perfect CSI is available at the receiver; however, acquiring perfect CSI at the receiver requires sending known pilot signals to the receiver to "train" it to learn the CSI, and this can take a long time especially when the number of antennas is large. If the time it takes for the receiver to learn the channel is only a negligible portion of the channel *coherence time*, then it is justifiable to put the effort to learn the channel. However, when the channel is changing rapidly and training takes a significant fraction of the channel coherence time, it is not worth it to acquire CSI that will change before enough information is sent to justify the time spent learning the channel. Hence, it is important to design space-time signaling schemes that are able to adapt with the current state of the channel between the transmitter and receiver, such that information can be communicated efficiently regardless of the availability of CSI. Space-time codes designed for the scenario of perfect CSI at

the receiver are called *coherent* codes; while, codes designed to work when no CSI is available at the receiver are called *noncoherent* codes.

Noncoherent MIMO was recognized by the European Union project "Mobile and wireless communications Enablers for the Twenty-twenty Information Society (METIS)" [38] as one of the enabling technologies for the future fifth generation (5G) mobile networks.

In the rest of this chapter, we provide the necessary background on wireless MIMO communications in general, and review the exiting literature.

1.2 The Wireless Channel

Wireless communication systems offer the freedom of untethered connectivity between communicating devices without the need for costly wires and infrastructure. However, ensuring reliable high speed wireless connectivity is a daunting task. The system designer has to take into consideration the hostile nature of the wireless channel. An accurate model of the wireless channel is needed to design systems that will perform well in practice. To accurately model the wireless channel, one must take into account the inherent way by which the information carrying electromagnetic waves propagate between the communicating terminals. In particular, electromagnetic waves emitted from the transmitter impinge on various objects and reflect off them to travel along different paths to reach the receiver. Those signal waves that traveled along different paths will attenuate by different amounts and undergo different phase rotations and time delays. When two or more multipath components arrive a similar time they will combine either constructively, or destructively and

this will cause what appears to be random fluctuations on the received signal power. These random fluctuations give rise to what is widely known as the *fading* phenomenon [28] [7], which is one of the key nuisances in wireless channels. Moreover, if the paths taken by different wave components differ significantly in length, different signal components may experience large enough delay such that components from different symbols interfere together which lead to what is known as *inter-symbol interference* [28].

The *fading* phenomenon resulting from multipath propagation is not the only nuisance in wireless channels. Unlike wireline communications, where the link between the transmitter and the receiver is an isolated point-to-point link, the wireless medium is shared by a large number of other users and services, which may be operating in the same frequency band and can cause significant *interference* at the receiver and deteriorate the reliability of reception.

Despite of the negative effects, discussed earlier, that multipath propagation can have on wireless links performance, it can also be beneficial under certain conditions. Suppose the transmitter can launch several copies of the information signal through different paths to the receiver. If we ignore the interference and assume all paths are independent and can be separated at the receiver. Thus each path can be thought of as a separate channel. Even if any of these paths suffers from deep attenuation, the rest of the paths can provide a detectable signal to the receiver. This will increase the reliability of the link and improve error performance. Another way to exploit multipath, is to increase the data rate by sending multiple streams of data from the transmitter along the different paths. Hence, multiple path propagation can be exploited to either improve the reliability of the wireless

link or to increase the transmitted data rate and thus improve spectral efficiency [7]. The former gain is called *diversity gain*, and the latter is called *multiplexing gain*. It is worth mentioning that these two gains are not mutually exclusive, and there exists a fundamental tradeoff between how much of each a gain a coding scheme can get [48].

1.3 Multiple Antenna Wireless Systems

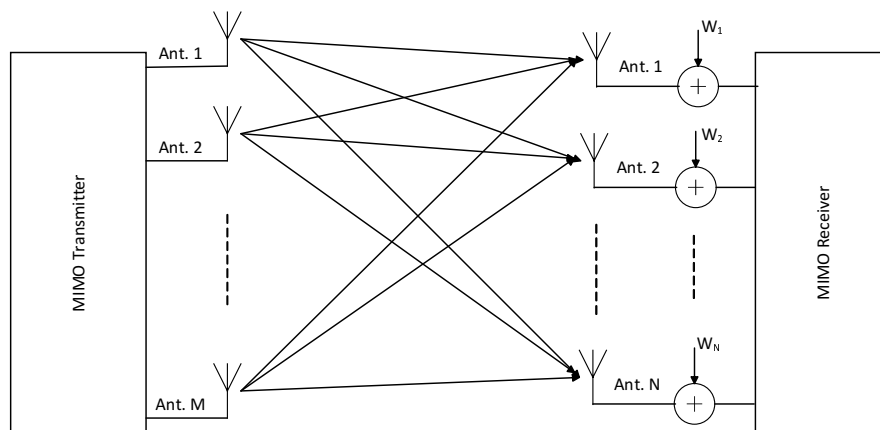


FIGURE 1.1: Multiple Antenna Communication System

One way to exploit the potential benefits of multipath propagation is to use multiple antennas both the transmitter and the receiver. By employing multiple antennas at the transmitter and the receiver, information can be propagated in different paths in a controlled manner. Consider a communication system where the transmitter has M antennas and the receiver has N antennas. Such a system is generally called a multiple-input multiple-output (MIMO) communication system. This system is depicted in Figure 1.1. The arrow between the i -th transmit antenna and the j -th receive antenna denote the ij -th signal path. In general, each signal path consists of several

subpaths [28], and the received signal from the ij -th path is the superposition of the constituent subpaths. That being the general case, each signal path can be thought of as a finite impulse response filter that characterizes the channel impulse response of this path. In the special case, when the bandwidth occupied by the transmitted signal is smaller than the coherence bandwidth of the channel, the frequency response of the ij -th path channel is essentially constant over the signal bandwidth, and the channel is said to be frequency flat or frequency non-selective. In this case, the multipath components cannot be resolved, and the complex gain function of the channel can be well approximated by a complex-valued scalar. On the other hand, if the transmitted signal bandwidth is larger than the coherence bandwidth of the channel, then the approximation used earlier is not valid, and the channel is said to be frequency-selective. However, a wide-band signal can be decomposed into narrow subbands components such that the frequency-flat model is justifiable within each subband [11] [32] [42]. This is the approach used in multicarrier systems like *Orthogonal Frequency Division Multiplexing (OFDM)*. Therefore, the frequency-flat assumption is reasonable for a wide variety of practical systems. Throughout this thesis we will restrict our attention to frequency flat channels where the complex gain functions are assumed to be complex-valued scalars.

The complex gain functions of the wireless channel can change over time depending on the propagation environment and mobility of the transmitter and the receiver. Wireless channels are characterized based on how fast their complex gain functions change over time. When the channel gain function changes within one symbol duration, the channel is said to be a fast-fading channel. On the other hand, if the channel gain functions remain unchanged for more than

one symbol duration, the channel is said to be a slow-fading channel. Through out this thesis, we will assume the channel is a slowly-fading frequency-flat channel. This class of channels include block-fading channel. In a block fading channel, the channel gain functions remain constant for several symbol periods and then change independently to new realizations. The time during which the channel remains constant is called the coherence time or coherence interval. The coherence time is an important factor in deciding which signaling scheme to use in a given communication scenario.

In addition to nuisance caused by fading, the received signal is also affected by thermal noise. Thermal noise results from the random motion of electrons in the electronic devices used in signal reception and processing. To model the affect of thermal noise, an additive stochastic term is added to the received signal. This term is statistically independent from both the transmitted signal and the propagation parameters of the wireless channel. In Figure 1.1, W_j represents the noise term at the j -th receiving antenna.

To utilize the full potential of multiple antennas propagation, different receive antennas must provide us with diverse and independent representations of the transmitted signals. For that to happen, the wireless channel must be richly scattered. In a richly scattered environment, the complex path gains of different paths are statistically independent. Therefore, signals traveling along different paths suffer from independent fading. Hence, the receiver is provided with diverse statistically independent versions of the information carrying signal. On the other hand, if the channel is not richly scattered, complex path gain are statistically dependent resulting in similar fades in different paths, and the receiver gets less diverse versions of the information carrying signal. In a richly scattered environment,

independent fading is approximately achieved by adequate antenna elements separation. Field measurements conducted showed that typical adequate antenna separation should be between 0.5λ and 10λ , where λ is the wavelength of the carrier [12] [31]. At typical radio frequencies, this corresponds to a few centimeters separation between antenna elements. These separations could be easily achieved in typically available space at the transmitter and/or receiver. Hence, throughout the rest of this thesis, the channel is assumed to be richly scattered, and thus the path gains are independent.

1.4 Space-Time Coding

In conventional wireless communication systems, there is a single antenna element at the transmitter, and the data is encoded over the time axis. However, in MIMO systems, the transmitter has multiple antenna elements, and the data is encoded temporally over the time axis and spatially over the antenna indices. The time axis is usually partitioned into time slots where each time slot represent a channel use. Such that every codeword is a matrix where each entry is a space-time slot representing a specific antenna element and time slot.

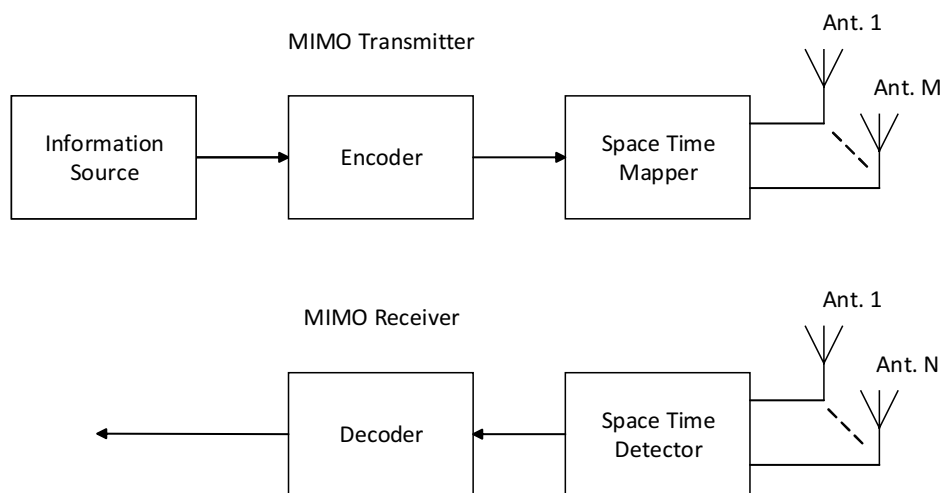


FIGURE 1.2: Generic MIMO Communication System

Figure 1.2 shows a generic MIMO communication system. In the transmitter, raw information bits are encoded and divided into blocks. Then each block of encoded bits is mapped to a corresponding space-time channel symbol [4]. Each space-time channel symbol is assigned a particular set of signaling waveforms represented in baseband by a complex matrix. The set of all possible matrices representing all potential space-time channel symbols is called a space-time code or codebook [4]. Finally, the signaling waveforms representing the space-time channel symbol being transmitted is then amplified and propagated from their corresponding antennas at their respective time slots. At the receiver, the processing done at the transmitter is reversed. The space-time detector decides on the best estimate of the transmitted signaling waveforms, and then the received signaling waveforms are demapped back to the encoded bits. Lastly, a decoder is used to retrieve the original raw information bits.

The design of the space-time signaling waveforms depends on the nature of the channel. One important parameter of the channel that governs the choice of the suitable signaling strategy is the coherence time of the channel. Recall that the coherence time of a wireless channel is the time during which the channel response remains unchanged. If the coherence time of the channel is sufficiently long [42], the transmitter could send pilot signals which are known to the receiver, and the receiver can use these signals to estimate the channel response. Moreover, if the length of the coherence time permits, the receiver can send the estimated channel response to the transmitter via a separate feedback channel. Equipped with knowledge of the channel response, the transmitter can optimize its coding strategy to maximize the amount of information communicated to the receiver. The receiver also uses the channel knowledge to perform reliable and

efficient detection of the transmitted information. For a sufficiently long coherence time, it can be assumed that the time spent estimating the channel response and sending it back to transmitter is a negligible portion of the coherence time, and the remaining portion of the coherence time is spent sending information. Hence, we can reasonably model the system as if the channel is known to both transmitter and receiver before transmission begins. This scenario requires resources that are usually difficult to accommodate [16]. In particular, the availability of a separate feedback channel cannot always be guaranteed; furthermore, if such a channel is available, the coherence time has to be long enough for the receiver to feedback the channel response to the transmitter, which is typically not the case in practical situations where mobility of the transmitter and/or receiver causes the channel to change rapidly. Given the impracticalities of realizing this scenario, a more practical communication model is typically used. In this model, the transmitter also sends pilot signals for the receiver to estimate the channel response, and it is assumed the receiver is able to estimate the channel response perfectly; however, the receiver does not share channel knowledge with the transmitter. This model eliminates the need for a feedback channel and lessens the requirements on coherence time. This communication model is usually referred to as coherent in literature [34]. In coherent communication models, the amount of time required to acquire an estimate of the channel at the receiver through the use of pilot signals is assumed to be a negligible portion of the coherence time of the channel; thus, it is reasonable to assume that the receiver knows the channel before transmission of information. A brief overview of codes that are used with coherent MIMO communication systems is given in section 1.6.2.

In some practical situations, the amount of time required to acquire an accurate estimate of the channel at the receiver is a significant portion of the coherence time of the wireless channel. This problem is more pronounced when the transmitter and/or receiver are moving rapidly or when the number of antennas at the transmitter and/or receiver is large [48] which requires sending a lot of pilot signals to estimate the channel. In such situation, it is more practical to assume that neither the transmitter nor the receiver know the channel before transmission. This communication model is referred to as non-coherent [34]. We can still send pilot signals and estimate the channel at the receiver in this type of communication models; however, the amount of time required for that has to be taken into consideration. Codes that is used with non-coherent MIMO communication systems are briefly introduced in section 1.6.1.

1.5 System Model

In this section, we formally introduce the space-time communication model that will be used throughout this thesis. A space-time signaling scheme consists of a set of waveforms that are localized in a specific space-time slot, that is; each waveform is transmitted from a specific antenna in a specific time slot. The information-carrying waveform that is transmitted from the j -th antenna in the i -th time slot can be written as $s_{ij}(t)$. The signal space occupied by these information carrying waveforms $\{s_{ij}(t)\}$ can be represented by a set of orthogonal functions $\{\phi_k(t)\}$ that form a basis for this signal space. Hence, any signal in this signal space can be expressed as a linear combination of the basis signals $\{\phi_k(t)\}$, and we may write $s_{ij}(t) = \sum_k s_{ij}^k \phi_k(t)$. A typical choice for the basis functions is the

quadrature sinusoidals $\sin 2\pi f_c t$ and $\cos 2\pi f_c t$, where f_c is the RF carrier frequency. In this case, each waveform can be expressed as a complex scalar representing the amplitude and phase of the transmitted sinusoid.

In practical communication systems, the transmitted waveform has to be shaped to make it better suited to the communication channel. In particular, the transmitted waveform has to meet the limitations of the available channel bandwidth, and be resilient to timing error caused by imperfect synchronization at the receiver. To achieve these goals, a pulse shaping waveform $g(t)$ is used. The pulse shaping waveform is independent of the space-time slot and the information carrying waveform. A typical pulse shape is the root-raised cosine waveform. The root-raised cosine pulse shape satisfies the Nyquist criteria for zero *inter-symbol interference* (ISI) and is quite resilient to small timing errors at the receiver [28]. The transmitted waveforms, after pulse shaping, can be expressed as $x_{ij}(t) = s_{ij}(t)g(t)$.

In space-time signaling schemes, where the quadrature sinusoidal basis is used, the information carrying complex scalars s_{ij} comprising the space-time symbol have to possess some structure to achieve desirable properties. These desirable properties typically include resilience to adverse channel effects, support for high data rates transmission, and ease of detection.

Throughout this thesis, we consider the case where the quadrature sinusoidal basis is used, and the transmitted waveforms are represented using complex scalars s_{ij} . We let M denote the number of transmitter antennas and N denote the number of receiver antennas. In addition, the coherence interval of the channel is assumed to

span T time slots or channel uses. Given this scenario, any particular transmitted space-time symbol/codeword can be expressed as a $T \times M$ complex-valued matrix \mathbf{S} . The set of possible space-time codewords comprises the space-time codebook \mathcal{S} . The space-time mapper maps each block of encoded bits to a corresponding space-time codeword from the codebook.

As previously mentioned, we also restrict ourselves to the flat fading and richly scattered channels; hence, the channel complex gain functions between pairs of transmit and receive antennas are independent and identically distributed complex scalars h_{ij} . Therefore, the channel gain functions can be expressed as a complex-valued $M \times N$ matrix. The $T \times N$ received matrix \mathbf{Y} is given by

$$\mathbf{Y} = \mathbf{S}\mathbf{H} + \mathbf{W}, \quad (1.1)$$

where $\mathbf{S} \in \mathcal{S}$ and \mathbf{W} is the $T \times N$ matrix containing the noise samples. The noise samples are assumed to be i.i.d. zero-mean complex Gaussian random variables. Apart from scaling factors, this generic model is used throughout this thesis.

1.6 Literature Review

1.6.1 Noncoherent MIMO Codes

In this section we review the existing literature on noncoherent codes for the MIMO channel. By noncoherent codes, we mean codes that are decodable without knowledge of channel coefficients at the receiver. Research on space time codes that do not require channel state information at the receiver was motivated by the information theoretic works of Marzetta [34] and Zheng [49]. Marzetta

and Hochwald [34] were able to characterize the structure of the capacity achieving signals. It was shown that the capacity of the non-coherent MIMO channel can be achieved by using signaling matrices that are the product of an isotropically distributed (i.e. whose distribution is invariant to rotations) unitary matrix and an independent random diagonal matrix whose entries are real and non-negative. Moreover, at sufficiently high SNRs, the diagonal matrix elements become deterministic, and the information is almost exclusively carried by the unitary component. This led to a surge of research in "space-time unitary modulation" which is asymptotically optimal at high SNRs. In [49], Zheng and Tse computed the asymptotic capacity at high SNRs in terms of the number of transmit antennas M , the number of receive antennas N , and the coherence time T . The capacity gain for every 3 dB increase in SNR turned out to be $M^* (1 - \frac{M^*}{T})$ bits/channel use, where $M^* = \min(M, N, \lfloor T/2 \rfloor)$. On the other hand, the capacity gain of the coherent MIMO channel is $\min(M, N)$ for every 3 dB increase in SNR. They also gave a geometric interpretation of the capacity expression as sphere packing on the compact Grassmann manifold $\mathbb{G}(T, M)$ [45]. The Grassmann manifold is the set of all M -dimensional subspaces in \mathcal{C}^T . An intuitive explanation of this result can be given as follows, at very high SNRs, the received matrix is approximately $\mathbf{Y} = \mathbf{S}\mathbf{H}$, and thus the subspace spanned by the received matrix \mathbf{Y} is the same as the one spanned by the transmitted matrix \mathbf{S} . Hence, if we design the constellation such that the different points span different subspaces, we will be able to decode transmitted constellation points without needing to have knowledge of the channel coefficients in \mathbf{H} . These constellations are called unitary or Grassmannian constellations in literature.

Several approaches for designing non-coherent Grassmannian constellations were proposed in literature. These approaches fall mainly into two categories. In the first category, constellations are designed by numerical optimization of some measure of distance between constellation points to maximize separation between points [15] [6], or by numerical minimization of some bound on error probability [36]. In the second category, noncoherent Grassmannian codes are synthesized from coherent codes using either an algebraic construction [18] [47] [46] [43] or a mapping to the Grassmannian manifold [22] (e.g. the exponential map [45]). For example, in [22], the authors used the fact that the tangent space of the Grassmannian manifold $\mathbb{G}_M(\mathbb{C}^T)$ at an arbitrary point \mathbf{G} is given by the set of matrices

$$\Delta = \mathbf{G} \begin{pmatrix} \mathbf{0} & \mathbf{V} \\ -\mathbf{V}^\dagger & \mathbf{0} \end{pmatrix}, \quad (1.2)$$

where $\mathbf{V} \in \mathbb{C}^{M \times (T-M)}$, and that any point on $\mathbb{G}_M(\mathbb{C}^T)$ can be obtained from points on the tangent space by an exponential mapping. Such that, all points on $\mathbb{G}_M(\mathbb{C}^T)$ can be obtained using the form

$$\mathbf{X} = \left[\exp \begin{pmatrix} \mathbf{0} & \mathbf{V} \\ -\mathbf{V}^\dagger & \mathbf{0} \end{pmatrix} \right] \mathbf{I}_{T,M}, \quad (1.3)$$

where $\mathbf{I}_{T,M} = [\mathbf{I}_M \mathbf{0}_{T-M}]^\dagger$. On the other hand, in [18], constellation points are constructed by successively rotating an initial unitary $T \times M$ representing an M -dimensional in a higher-dimensional complex space. Both categories of design approaches have their advantages and drawbacks. Generally, constellations designed by numerical optimization techniques exhibit superior performance; however, these constellations do not possess any particular structure rendering their

storage and detection cumbersome. These problems become more pronounced for large cardinalities (i.e. sizes), which are typically desirable at high SNRs. On the other hand, constellations designed by algebraic construction and mappings are amenable to more efficient storage and detection techniques, but suffer from performance degradation compared the first category.

Aside from unitary/Grassmannian constellation, "training-based" scheme was also proposed in literature for noncoherent MIMO communications [17] [8] [14]. Although these codes are called "noncoherent" in literature, training is used in these schemes to estimate the channel coefficients. However, the time spent training the receiver is taken into consideration, and the channel coefficients are not assumed to be known before transmission to the receiver, which fit the system model used in literature when studying noncoherent MIMO codes. Transmission over the channel coherence interval is divided into two phases, a training phase where pilots are sent to estimate the channel, and coherent a communication phase where information is sent. These codes attains the maximum degrees of freedom at high SNRs, however; they do not achieve full capacity [49].

For sake of completeness, we briefly review the design of coherent MIMO codes in the next section

1.6.2 Coherent Codes

Considering the scenario that the receiver has accurate CSI. The channel is assumed to be a block-fading Rayleigh fading channel described earlier, where channel matrix elements are iid Gaussian and change independently to a new realization for every space-time

codeword. The optimal coherent decoder uses the well known ML rule and the estimated codeword is given by:

$$\hat{\mathbf{S}} = \arg \min_{\mathbf{S}} \left\| \mathbf{Y} - \sqrt{\frac{E_s}{M}} \mathbf{S} \mathbf{H} \right\|, \quad (1.4)$$

where E_s is the total average energy transmitted, and M the number of transmit antennas.

Design Criteria

Given that the ML rule is used at the receiver to estimate the transmitted codeword, the probability that the receiver decides in favour of the wrong codeword $\mathbf{S}^{(j)}$ given that $\mathbf{S}^{(i)}$ was transmitted can be upper bounded by the following expression [44]:

$$P(\mathbf{S}^{(i)} \rightarrow \mathbf{S}^{(j)}) \leq \left(\prod_{k=1}^r \lambda_k(i, j) \right)^{-N} \left(\frac{E_s}{4N_0} \right)^{-rN}, \quad (1.5)$$

where $\lambda_k(i, j)$'s and r are, respectively, the real non-negative eigenvalues and the rank of the matrix $\mathbf{A} = (\mathbf{S}^{(j)} - \mathbf{S}^{(i)}) (\mathbf{S}^{(j)} - \mathbf{S}^{(i)})^\dagger$, where $(\cdot)^\dagger$ denotes the Hermitian (conjugate transpose). This leads to the two well known *Rank Criterion* and *Determinant Criterion* [44].

- *Rank Criterion*: the diversity gain of a space-time code depends on the term $\left(\frac{E_s}{4N_0} \right)^{-rN}$. Hence, for any space-time code to achieve full spatial diversity order of MN , the difference matrix \mathbf{A} must be full rank for all possible pairs of codewords in the code.
- *Determinant Criterion*: the coding gain of a space-time code depends on the term $\left(\prod_{i=1}^r \lambda_i \right)^{-N}$. Hence, to maximize coding gain, the code must be designed such that the minimum of

the determinant of the matrix \mathbf{A} is maximized over all possible pairs of codewords.

Before moving on, it is worth mentioning one example of coherent codes, the famous Alamouti orthogonal space-time block code (OSTBC) [3]. In the Alamouti scheme, the transmitted space-time codeword may be expressed as

$$\mathbf{S} = \begin{bmatrix} s_1 & -s_2^* \\ s_2 & s_1^* \end{bmatrix}, \quad (1.6)$$

where s_1 and s_2 are drawn from any APM (amplitude phase modulation) constellation. The difference matrix between any two codewords $\mathbf{E}_{i,j} = \mathbf{S}^{(j)} - \mathbf{S}^{(i)}$ will take the form:

$$\mathbf{E}_{i,j} = \begin{bmatrix} e_1 & -e_2^* \\ e_2 & e_1^* \end{bmatrix}, \quad (1.7)$$

Obviously, the difference matrix is orthogonal, and hence $\mathbf{A} = \mathbf{E}_{i,j} \mathbf{E}_{i,j}^\dagger$ has full rank (i.e. $r = M = 2$) [24]. In general the Alamouti scheme achieves a full diversity order of $2N$. Moreover, the unique structure of the code renders the effective channel matrix orthogonal [3], which reduces the complex vector ML detection problem into two simpler scalar detection problems.

1.7 Thesis Outline and Contributions

In this thesis, we propose space-time coding techniques for two scenarios. In the first scenario, we consider a point-to-point noncoherent MIMO channel, and in the second scenario; we consider a multicast MIMO channel with coherent and noncoherent receivers.

Throughout this thesis, it is assumed that CSI is not available at the transmitter. The rest of this thesis is organized as follows.

In chapter 2, we propose a new approach to design non-coherent MIMO codes. Unlike designs in literature where number of active transmit antennas during any signaling interval is chosen to maximize the degrees of freedom used, we let the number of active transmit antennas vary across constellation points to improve performance at low-to-moderate SNRs where the system is not limited by the degrees of freedom. We design Grassmannian constellations of different dimensions by direct numerical optimization [15] on the Grassmannian manifold. The designed constellations are then augmented with points from a one-dimensional constellation that are chosen to maximize the minimum distance of the augmented constellation. We use numerical simulations to show that our designed codes exhibits superior performance, compared to existing noncoherent codes designed by direct numerical optimization or exponential mappings [22], at low-to-moderate SNRs without sacrificing performance at higher SNRs up to 25 dB.

In chapter 3, a multi-layer coding scheme for the MIMO multicast channel is considered [19, 20, 21] [29, 30]. The proposed scheme combines noncoherent Grassmannian MIMO codes with spatial modulation (SM) [37]. Two classes of receivers are considered; one class of receivers are able to acquire CSI, and the other class are unable to acquire CSI. Information is encoded in two layers; we encode basic low resolution (LR) information using noncoherent Grassmannian MIMO codes which all receivers should be able to decode, and incremental high resolution (HR) information is encoded in the indices of the transmit antennas used to transmit the Grassmannian codeword, and only receivers with CSI knowledge are able to decode it.

Furthermore, We propose a two step decoder that is more computationally efficient than the optimal decoder. Simulation results suggest that the proposed coding scheme for the high-resolution layer outperforms existing space-time codes synthesized from APM constellations [20], and those obtained by direct numerical optimization on the unitary group [21].

Finally, in chapter 4, we conclude this thesis and suggest few directions for future work.

Chapter 2

Non-coherent Grassmanian

MIMO Codes for

Low-to-Moderate SNRs

In this chapter, we propose a new approach to construct space-time codes for multiple-input multiple-output (MIMO) noncoherent channel. Unlike designs which fixed the number of transmit antennas M , which was chosen to utilize all the complex degrees of freedom of the system (i.e. $M = \min(\lfloor \frac{T}{2} \rfloor, N)$, where T is the coherence interval of quasi-static Rayleigh fading channel, and N the number of receive antennas, in our designs we let the number of the transmit antennas be a variable m which could take any value from 1 to $M = \min(\lfloor \frac{T}{2} \rfloor, N)$ over constellation points. We use numerical simulations to evaluate the performance of our proposed designs. At low-to-moderate SNRs, where the system is not limited by the degrees of freedom used, simulations results show that our codes could provide significant performance gains over codes designed using direct numerical optimization and exponential mappings [22] where the number of transmit antennas is fixed, especially at higher constellation cardinalities. Moreover, there is no discernible loss in performance at higher SNRs up to 25 dB from not utilizing the maximum

number of degrees of freedom.

2.1 Introduction

Multiple-input multiple-output (MIMO) communication systems operating in a Rayleigh fading environment promise significant gains in capacity over single antenna systems. However, to reap the benefits of MIMO communications, like higher capacity or lower error rate, the channel fading coefficients must be statistically independent and known to the receiver. Acquiring accurate channel state information (CSI) becomes increasingly difficult if the number of antennas becomes too large, the channel is changing rapidly, or when traffic is bursty in nature and communication resources are too valuable to waste estimating the channel instead of sending data as is the case in the emerging area of Internet of Things.

Considering the difficulties of acquiring accurate CSI, non-coherent MIMO systems become an attractive option in various scenarios. Non-coherent MIMO systems do not rely on accurate CSI at the receiver nor at the transmitter. It has been shown in [34], that the capacity of the non-coherent MIMO link is achieved when the $T \times M$ transmitted signal matrix, where T is the coherence interval of the channel and M the number of transmit antennas, is the product of an isotropically distributed $T \times M$ unitary matrix and an independent random diagonal matrix D whose entries are real and non-negative. This structure achieves the capacity regardless of the received SNR, and channel coherence interval T . Designing non-coherent constellations that are optimal both at low and high SNRs is still an open problem. For example, at high SNRs, the capacity achieving input signals is isotropically distributed unitary matrices [35] [49] (i.e., $D = \mathbf{I}_M$) provided

that $T \geq \min(M, N) + N$, where N is the number of receive antennas, while at low SNRs [41], only one entry of D is non zero, and the optimal number of transmit antenna M is one.

In literature, the majority of constellation designs for non-coherent MIMO channel assumes the communication system operates at high SNRs, and seek to use all the degrees of freedom, $M(1 - \frac{M}{T})$ bits per seconds per hertz [49], of the system, where $M = \min(\lfloor \frac{T}{2} \rfloor, N)$ is the required number of transmit antennas to attain the maximum number of degrees of freedom. These constellations are packings on the complex Grassmann manifold, and are designed either numerically by maximizing some measure of distance between constellation points [15] [6], using algebraic construction [46], or by using parameterized mappings [22] [47]. On the other hand, constellation designs that are more appropriate for low SNR were proposed in [1], where the Kullback-Leibler distance metric is used to design multi-level unitary constellations (orthogonal) more suitable at low SNRs. However, the structure of the constellations designed in [1] depends on the value of the SNR, and a separate constellation has to be designed for each SNR value.

In the following sections, we design space-time block codes for the non-coherent MIMO channel that perform better than conventional unitary constellations designed to exploit all the degrees of freedom of the system, at low SNR, without sacrificing performance at practical higher SNRs. Guided by information theoretic results that using only one transmit antenna is optimal at low SNRs [41], we let the number of transmit antennas used be variable across the constellation. In our designed constellation, the points are either one-dimensional vectors or $T \times M$ matrices where M is the required number of antenna to exploit all the degrees of freedom of the system.

Simulation results show that our designs exhibit performance superior to constellations in [15] and [22] at low-to-moderate SNRs.

2.2 Preliminaries and System Model

2.2.1 The Grassmann Manifold

Consider the set of all $T \times M$ unitary matrices for $T \geq M$. This set defines the Stiefel manifold $\mathbb{S}_{T,M}$ of dimension $T \times M$. Define an equivalence relation where two points \mathbf{P} and \mathbf{Q} on the Stiefel manifold are equivalent if their T -dimensional column vectors span the same subspace. In other words, $\mathbf{P} \equiv \mathbf{Q}$ if they are related by right multiplication of a unitary matrix Ω such that

$$\mathbf{P} = \mathbf{Q}\Omega, \quad \Omega \in \mathbb{U}_M, \quad (2.1)$$

where \mathbb{U}_M is the unitary group consisting of all $M \times M$ unitary matrices. The Grassmann manifold $\mathbb{G}_M(\mathbb{C}^T)$ is defined as the quotient manifold of the Stiefel manifold $\mathbb{S}_{T,M}$ with respect to the equivalence relation in (2.1). Every point on the Grassmann manifold is an equivalence class in the Stiefel manifold. For more details, consult any standard textbook (e.g. [45]).

2.2.2 Chordal Frobenius Distance

Constellation design requires an appropriate metric to measure the distance between constellation points. It was shown in [15], based on an analysis of how the noise perturbs the subspace spanned by the transmitted signal point, that the chordal Frobenius norm is an

appropriate metric to measure distance between points on the Grassmann manifold. Given two constellation points \mathbf{S}_i and \mathbf{S}_j , the chordal Frobenius norm between them is defined as

$$d(\mathbf{S}_i, \mathbf{S}_j) = \sqrt{2M - 2 \text{Tr}(\boldsymbol{\Sigma}_{\mathbf{S}_i^\dagger \mathbf{S}_j})}, \quad (2.2)$$

where $\mathbf{S}_i^\dagger \mathbf{S}_j = \mathbf{U}_{\mathbf{S}_i^\dagger \mathbf{S}_j} \boldsymbol{\Sigma}_{\mathbf{S}_i^\dagger \mathbf{S}_j} \mathbf{V}_{\mathbf{S}_i^\dagger \mathbf{S}_j}$ is the singular value decomposition (SVD) of $\mathbf{S}_i^\dagger \mathbf{S}_j$ [13]. We adopt the chordal Frobenius norm as a measure of distance between signal points in our designs.

2.2.3 System Model

A MIMO channel is considered. The transmitter has M antennas, and the receiver has N antennas. The channel is assumed to be a quasi-static Rayleigh flat fading MIMO channel, and the noise is additive white Gaussian noise. The system can be modeled as

$$\mathbf{Y} = \mathbf{S}\mathbf{H} + \sqrt{\frac{M}{\rho T}} \mathbf{W}, \quad (2.3)$$

where \mathbf{Y} is the $T \times N$ received matrix at the receiver. \mathbf{S} is the $T \times M$ transmitted codeword matrix. \mathbf{H} denote the $M \times N$ channel matrix between the transmitter and the receiver and \mathbf{W} denote the $T \times N$ noise matrix at the receiver. The entries of the channel and noise matrices are independent, and identically distributed, circularly symmetric, complex Gaussian random variables with zero means and unit variances $\mathcal{CN}(0, 1)$. Finally, the SNR is given by ρ . The channel matrix entries are assumed to remain constant for the coherence interval T , and then change independently to a new realization. At the receiver, the maximum likelihood detector [34] is used.

2.3 Code Construction and Decoding

In [15] and [22], the number of transmit antennas M was chosen to maximize the number of degrees of freedom of the system for a given coherence interval T and number of receive antennas N

$$M^* = \min \left(\left\lfloor \frac{T}{2} \right\rfloor, N \right). \quad (2.4)$$

Maximizing the degrees of freedom is particularly useful at high SNRs, where the system is degrees-of-freedom limited. However, at lower SNRs, the system is power limited, and maximizing the degrees of the freedom will not necessarily lead to better error performance. Moreover, information theoretic results [49, 41] show that, in the case of unitary modulation, the optimal number of transmit antennas at low SNR is only one. The low-SNR mutual information for unitary modulation was calculated [41] to be

$$\frac{1}{T} I(\mathbf{Y}; \mathbf{S}) = \frac{N(T-M)}{2M} \rho^2 + o(\rho^2), \quad (2.5)$$

which is maximized by letting $M = 1$. These results were supported by our simulations, which showed that one-dimensional Grassmanian constellations performed better than M^* -dimensional Grassmanian constellations at lower SNRs. However, as the SNR increases, the system begins to be limited by the degrees of freedom, and the M^* -dimensional constellations start to perform better. This suggests that by letting the number of transmit antenna be a variable m which is not constant for the entire constellation and can take any value from 1 to M^* , we can design codes that perform better at low-to-moderate SNRs without incurring discernible performance loss at

higher SNRs. Following this argument, we augment an M^* -dimensional Grassmannian constellation with one-dimensional points, such that the transmitted signal matrices are either $T \times M^*$ unitary matrices or a $T \times M^*$ matrix where the first column represents a one-dimensional Grassmannian point and the rest of the entries equal to zero (e.g., $\mathbf{S} = [\mathbf{Q}_{T \times 1} \quad \mathbf{0}_{T \times (M^* - 1)}]$). We limit ourselves to points that are either one-dimensional or M^* -dimensional in this chapter because one dimension is optimal at low SNRs, while the other is optimal at high SNRs, but; in general, points with dimensions ranging from 1 to M^* can be used to design constellation with variable dimensions.

Our design approach starts with a initial M^* -dimensional Grassmannian constellation \mathcal{C}_M designed using the direct approach in [15] whose size is half of the desired constellation size $|\mathcal{C}|$. This constellation is then augmented with one dimensional points. One-dimensional points are selected one-by-one from a one-dimensional constellation, also designed using the direct method, \mathcal{C}_1 with high cardinality $|\mathcal{C}_1|$ to maximize the minimum chordal Frobenius distance with all previously added points. This will result in what we call *augmented* constellations, whose half of their points is one-dimensional and the other half is M^* -dimensional. Different ratios of one-dimensional and M^* -dimensional points could be used, but we limit ourselves to this case, because our trials showed that this case strike a compromise between low and high SNRs performance.

2.3.1 Initial Constellation Design

In this section, we briefly review the direct constellation design approach in [15] used to construct the multi-dimensional initial constellation and the one-dimensional constellation from which we augment the initial constellation. Using this approach, an entire constellation is jointly designed in one step. In particular, the $|\mathcal{C}|$ points on $\mathbb{G}_M(\mathbb{C}^T)$ are represented by a single point on $\mathbb{G}_{M|\mathcal{C}|}(\mathbb{C}^{T|\mathcal{C}|})$, and an analytical cost function that penalizes the pairwise chordal Frobenius distances between all constellation points is synthesized and numerically minimized using a derivative-based optimization algorithm [2] that automatically ensures all points remain on the surface of the Grassmann manifold after every iteration. The optimization problem can be written as:

$$\begin{aligned} & \min_{\{\mathbf{S}_k\}_{k=1}^{|\mathcal{C}|}} \max_{1 \leq i, j \leq |\mathcal{C}|} \text{Tr}(\boldsymbol{\Sigma}_{ij}) \\ & \text{subject to} \quad \mathbf{S}_k \in \mathbb{G}_M(\mathbb{C}^T), \quad k = 1, \dots, |\mathcal{C}|, \end{aligned} \quad (2.6)$$

where $\mathbf{U}_{ij} \boldsymbol{\Sigma}_{ij} \mathbf{V}_{ij}^\dagger$ is the singular value decomposition of $\mathbf{S}_i^\dagger \mathbf{S}_j$. The optimization problem in (2.6) has two issues; first, the objective function is non-differentiable because of the $\max(\cdot)$ function, and second, it is over multiple-points over the Grassmannian manifold at the same time. To solve the first issue, a refined Jacobian approximation [15] is used to obtain a smooth approximate representation, and to solve the second issue, the multiple points on $\mathbb{G}_M(\mathbb{C}^T)$ is represented as a single point on a manifold of higher dimension $\mathbb{G}_{M|\mathcal{C}|}(\mathbb{C}^{T|\mathcal{C}|})$. Hence,

the optimization problem can be rewritten as

$$\begin{aligned} & \min_{\{\mathbf{S}_k\}_{k=1}^{|\mathcal{C}|}} \left(\log \left(\sum_{i=1}^{|\mathcal{C}|-1} \sum_{j=i+1}^{|\mathcal{C}|} \exp(\text{Tr}^n(\boldsymbol{\Sigma}_{ij})) \right) \right)^{\frac{1}{n}} \\ & \text{subject to} \quad \mathbf{S}_k \in \mathbb{G}_M(\mathbb{C}^T), \quad k = 1, \dots, |\mathcal{C}|, \end{aligned} \quad (2.7)$$

where $n \geq 1$ is a parameter of the refined Jacobian approximation, such that as $n \rightarrow \infty$, the approximation approaches the exact value of the $\max(\cdot)$ function. Each matrix $\boldsymbol{\Sigma}_{ij}$ is expressed as

$$\boldsymbol{\Sigma}_{ij} = \mathbf{U}_{ij}^\dagger \mathbf{I}_M^{(i)} \bar{\mathbf{S}}^\dagger \left(\mathbf{I}_M^{(i)} \right)^\dagger \mathbf{I}_M^{(j)} \bar{\mathbf{S}} \left(\mathbf{I}_M^{(j)} \right)^\dagger \mathbf{V}_{ij}, \quad (2.8)$$

where $\bar{\mathbf{S}}$ is the $|\mathcal{C}|T \times |\mathcal{C}|M$ block diagonal matrix given by

$$\bar{\mathbf{S}} = \text{blkdiag}(\mathbf{S}_1, \dots, \mathbf{S}_{|\mathcal{C}|}), \quad (2.9)$$

and $\mathbf{I}_K^{(l)}$ denotes a fat block diagonal matrix with the l -th $K \times K$ block being the identity matrix \mathbf{I}_K and all other elements are equal to zero. Now by using (2.8), the optimization problem in (2.7) can be written as an optimization over the block diagonal matrix $\bar{\mathbf{S}}$. Because of its constrained structure, the matrix $\bar{\mathbf{S}}$ actually represent a point on a sub-manifold of $\mathbb{G}_{M|\mathcal{C}|}(\mathbb{C}^{T|\mathcal{C}|})$. It was shown in [15], that this sub-manifold inherits the canonical inner product and the projector from the parent manifold $\mathbb{G}_{M|\mathcal{C}|}(\mathbb{C}^{T|\mathcal{C}|})$, and that its tangent vectors posses the same block diagonal structure as $\bar{\mathbf{S}}$. This implies that if the optimization algorithm begins on a point in this sub-manifold, subsequent iterations will remain on the same sub-manifold. The conjugate gradient method in [2] can be used to minimize the cost function in (2.7) along geodesics of the manifold. To use the algorithm in [2], we need to find the gradient of the cost function derived

in (2.7). The gradient is defined on the Grassmann manifold as [2]

$$\nabla \mathbf{F} = \mathbf{F}_{\bar{\mathbf{S}}} - \bar{\mathbf{S}}\bar{\mathbf{S}}^\dagger \mathbf{F}_{\bar{\mathbf{S}}}, \quad (2.10)$$

where $\mathbf{F}_{\bar{\mathbf{S}}}$ is the matrix of partial derivatives which we computed to be

$$\mathbf{F}_{\bar{\mathbf{S}}} = \left(\log \left(\sum_{i=1}^{|\mathcal{C}|-1} \sum_{j=i+1}^{|\mathcal{C}|} e^{\text{Tr}^n(\boldsymbol{\Sigma}_{ij})} \right) \right)^{\frac{1}{n}-1} \frac{\sum_{i=1}^{|\mathcal{C}|-1} \sum_{j=i+1}^{|\mathcal{C}|} e^{\text{Tr}^n(\boldsymbol{\Sigma}_{ij})} \text{Tr}^{n-1}(\boldsymbol{\Sigma}_{ij}) \frac{d \text{Tr}(\boldsymbol{\Sigma}_{ij})}{d\bar{\mathbf{S}}}}{\sum_{i=1}^{|\mathcal{C}|-1} \sum_{j=i+1}^{|\mathcal{C}|} e^{\text{Tr}^n(\boldsymbol{\Sigma}_{ij})}}, \quad (2.11)$$

where the derivative $\frac{d \text{Tr}(\boldsymbol{\Sigma}_{ij})}{d\bar{\mathbf{S}}}$ can be calculated to be [39]

$$\begin{aligned} \frac{d \text{Tr}(\boldsymbol{\Sigma}_{ij})}{d\bar{\mathbf{S}}} &= \left(\mathbf{I}_M^{(i)} \right)^\dagger \mathbf{U}_{ij} \mathbf{V}_{ij}^\dagger \mathbf{I}_M^{(j)} \bar{\mathbf{S}}^\dagger \left(\mathbf{I}_T^{(j)} \right)^\dagger \mathbf{I}_T^{(i)} + \\ &\quad \left(\mathbf{I}_M^{(j)} \right)^\dagger \mathbf{V}_{ij} \mathbf{U}_{ij}^\dagger \mathbf{I}_M^{(i)} \bar{\mathbf{S}}^\dagger \left(\mathbf{I}_T^{(i)} \right)^\dagger \mathbf{I}_T^{(j)}, \end{aligned} \quad (2.12)$$

Now, we have everything we need to use the conjugate gradient algorithm in [2]. More details on this algorithm are covered in Appendix A.

2.3.2 Augmented Constellation

The M^* -dimensional constellation designed in section 2.3.1 is then augmented with one-dimensional points using Algorithm 1 to construct the final constellation \mathcal{C} . The algorithm takes as input two constellations; one is multi-dimensional with cardinality $|\mathcal{C}_M|$ which is half that of desired cardinality $|\mathcal{C}| = 2|\mathcal{C}_M|$, and the other one is one-dimensional with cardinality $|\mathcal{C}_1| \gg |\mathcal{C}_M|$. The multi-dimensional constellation is augmented with $|\mathcal{C}_M|$ points from the one-dimensional constellation sequentially. In particular, in each iteration, the pairwise distances between all one-dimensional in \mathcal{C}_1 and multi-dimensional

points in \mathcal{C}_M is calculated, and the one-dimensional point with the maximum minimum-distance from all points in the multi-dimensional constellation is added to the multi-dimensional constellation and removed from the one-dimensional constellation. This process is illustrated more clearly in Algorithm 1.

Algorithm 1 Algorithm for Augmented Constellation Design

Input: M-dimensional constellation \mathcal{C}_M and one-dimensional constellation \mathcal{C}_1

Output: Augmented Constellation

Initialisation :

- 1: **for** $i = 1$ to $|\mathcal{C}_M|$ **do**
- 2: **for** $j = 1$ to $|\mathcal{C}_1| + 1 - i$ **do**
- 3: **for** $k = 1$ to $|\mathcal{C}_M| - 1 + i$ **do**
- 4: Compute the distance $d_{j,k} = \sqrt{2M - 2 \text{Tr} \Sigma_{j,k}}$
- 5: **end for**
- 6: **end for**
- 7: Find the one-dimensional point that maximizes the minimum distance with all previous points.

$$\hat{\mathbf{S}}_j = \arg \max_j \min_k d_{j,k}$$

- 8: Add this one-dimensional point to multi-dimensional constellation.
 - 9: Remove this point from the one-dimensional constellation.
 - 10: **end for**
-

2.3.3 Decoder

The optimal noncoherent detector for the augmented constellation constructed in section 2.3.2 is the conventional non-coherent Maximum Likelihood (ML) decoder [34]. The probability distribution of the received matrix conditioned on the transmitted signal matrix can

be written as

$$p(\mathbf{Y}|\mathbf{S}) = \frac{\exp\left(-\text{Tr}\left(\mathbf{Y}^\dagger\left(\frac{M}{\rho T}\mathbf{I}_T + \mathbf{S}\mathbf{S}^\dagger\right)^{-1}\mathbf{Y}\right)\right)}{\pi^{TN}\det^N\left(\frac{M}{\rho T}\mathbf{I}_T + \mathbf{S}\mathbf{S}^\dagger\right)}. \quad (2.13)$$

The ML decoder searches over the entire constellation, \mathcal{C} , and decides in favour of the transmitted matrix that maximizes the expression in (2.13). It is worth mentioning that this decoder is not equivalent to the GLRT decoder given by $\hat{\mathbf{S}} = \arg \max_{\mathbf{S} \in \mathcal{C}} \text{Tr}(\mathbf{Y}^\dagger \mathbf{S} \mathbf{S}^\dagger \mathbf{Y})$ since the transmitted matrices are not always unitary in our case.

2.4 Simulation Results

In this section, numerical simulations are used to evaluate the performance of the proposed constellations. Our constellations are compared with the direct designed constellations from [15], and constellations constructed using exponential mapping [22]. In all simulations, the number of receive antennas N is two, and the channel coherence interval T is equal to four symbol durations. The maximum likelihood detector [34] is used, and the number of transmit antennas M depends on the constellation. For the constellations constructed using exponential mapping, we used the coherent code [22] given by

$$\mathbf{C} = \begin{bmatrix} s_1 + \theta s_2 & \phi(s_3 + \theta s_4) \\ \phi(s_3 - \theta s_4) & s_1 - \theta s_2 \end{bmatrix}, \quad (2.14)$$

where $\phi^2 = \theta = e^{i\frac{\pi}{4}}$ and s_i are drawn from QAM constellations whose size depend on the desired Grassmannian constellation cardinality. In all cases, the homothetic factors are chosen by numerical maximization of the minimal chordal product distance [22].

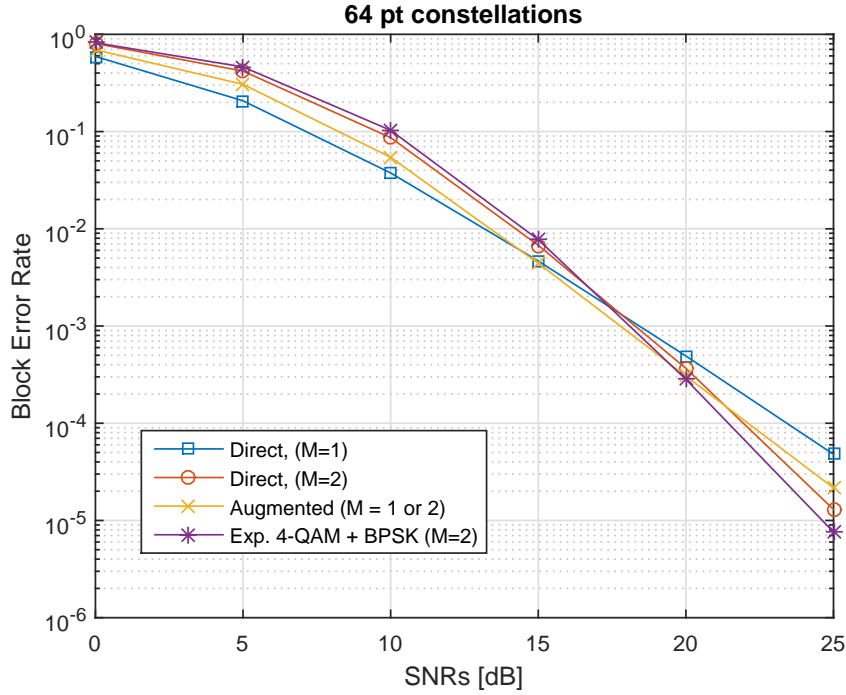


FIGURE 2.1: Performance of the augmented constellation against the ones in [15] (Direct, $M = 1$ and $M = 2$) and [22] (Exp.). For the Exp. constellation, s_1 and s_2 are drawn from 4-QAM const., where as s_3 and s_4 are drawn from BPSK const.

Figure 2.1 shows the error performance of the 64-point augmented constellation; superior performance over direct designed and exponentially mapped constellations with $M = 2$ is observed for SNRs up to 15 dB, while superior performance compared to direct designed constellation with $M = 1$ is observed over 15 dB. However, some degradation in performance is observed after 20 dB compared to designed and exponentially mapped constellations with $M = 2$ for this constellation size, which is expected, because we are not utilizing all the degrees of freedom of the system.

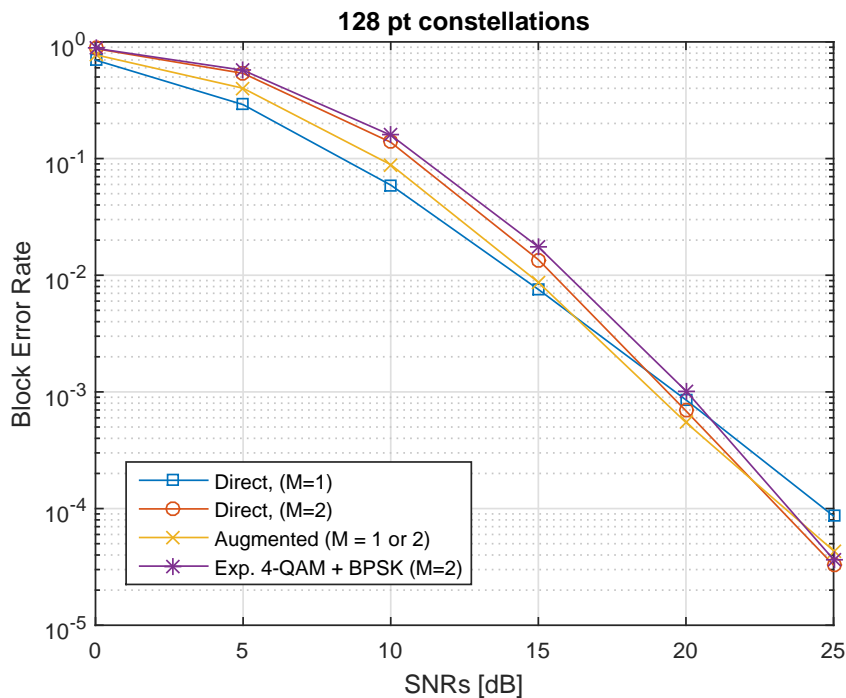


FIGURE 2.2: Performance of the augmented constellation against the ones in [15] (Direct, $M = 1$ and $M = 2$) and [22] (Exp.). For the Exp. constellation, s_1 , s_2 and s_3 are drawn from 4-QAM const., where as s_4 is drawn from BPSK const.

Figures 2.2 and 2.3 show the error performance for the 128 pt and 256 pt constellations respectively, where the augmented constellation exhibit better performance for low-to-medium SNRs up to almost 18 dB over direct designed and exponentially mapped constellations with $M = 2$. We also note there is no loss in performance for SNRs up to 25 dB compared to those constellations, and that the augmented constellations outperform one-dimensional (i.e. $M = 1$) direct designed constellations for SNRs over 17 dB. In general, as expected, the augmented constellations strike a compromise between one-dimensional and multi-dimensional constellations, where it performs better than multi-dimensional constellation for low-medium SNRs without significant loss in performance at higher SNRs where the system begins to be limited by the degrees of freedom.

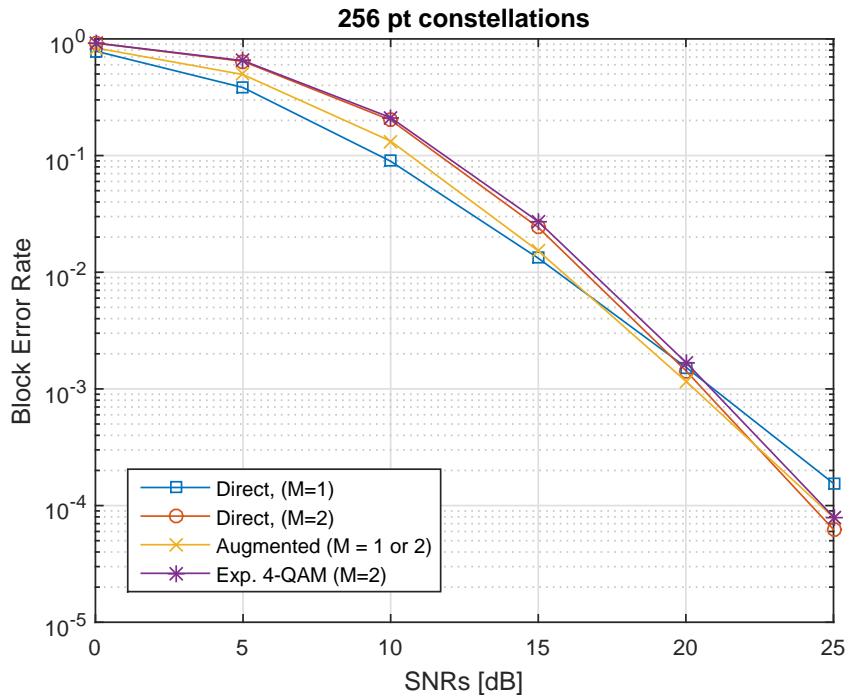


FIGURE 2.3: Performance of the augmented constellation against the ones in [15] (Direct, $M = 1$ and $M = 2$) and [22] (Exp.). For the Exp. constellation, s_1, s_2, s_3 and s_4 are drawn from 4-QAM const.

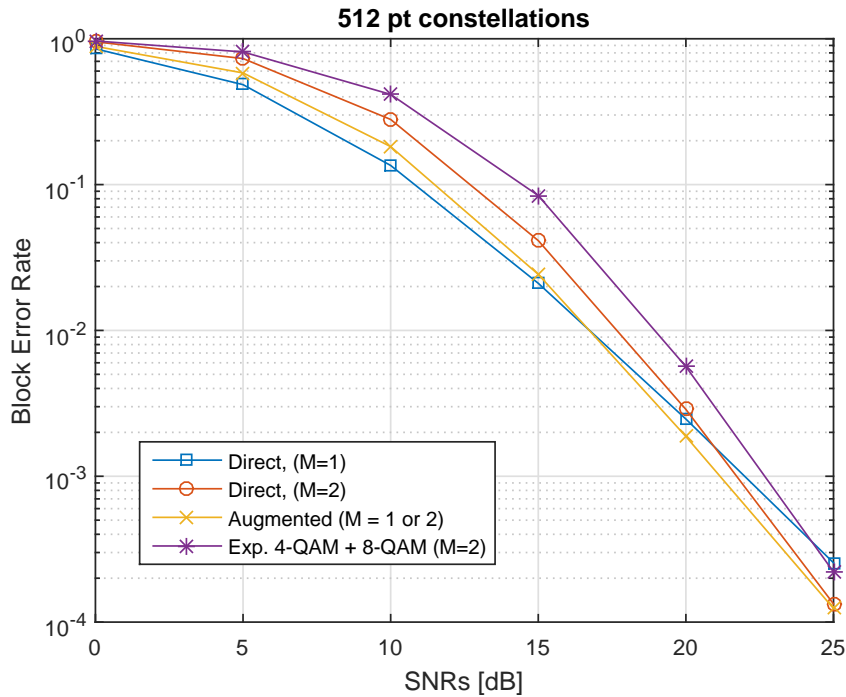


FIGURE 2.4: Performance of the augmented constellation against the ones in [15] (Direct, $M = 1$ and $M = 2$) and [22] (Exp.). For the Exp. constellation, s_2, s_3 and s_4 are drawn from 4-QAM const., where as s_1 is drawn from 8-QAM const.

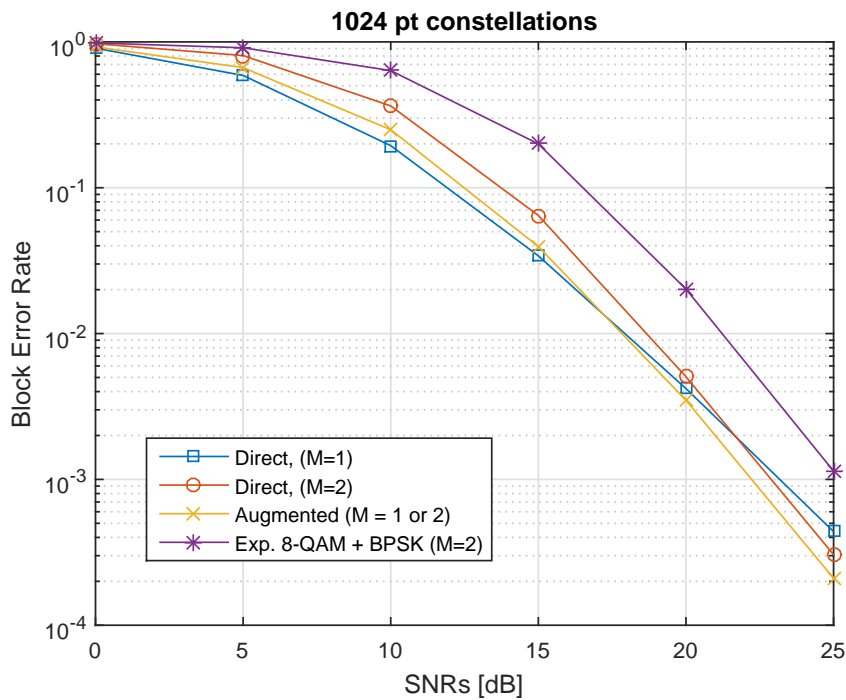


FIGURE 2.5: Performance of the augmented constellation against the ones in [15] (Direct, $M = 1$ and $M = 2$) and [22] (Exp.). For the Exp. constellation, s_1 , s_2 and s_3 are drawn from 8-QAM const., where as s_1 is drawn from BPSK const.

As the constellations grow in size, we note our designs show even better performance for a wider range of SNRs. This can be seen in figures 2.4 and 2.5 for the 512 points and 1024 points constellations, where gains over strictly multi-dimensional constellations can be seen all the way to an SNR of 25 dB.

Chapter 3

Multiresolution Multicasting using Grassmannian MIMO codes and Space Shift Keying

In this chapter, we consider layered space-time signaling over the multiple input multiple output multicast channel. In multi-resolution multicast MIMO systems, the transmitter sends multi-resolution information to multiple receivers. In the scheme we propose, information is encoded into two layers; low-resolution (LR) information which can be detected noncoherently, and high-resolution (HR) information which must be detected coherently. Depending on the mobility of the receiver and relative location from the transmitter, the receiver may not be able to acquire accurate CSI. Receiver that are not able to acquire CSI can still decode the basic low-resolution information, while receivers with CSI can also decode the incremental high-resolution information on top of the low-resolution information. In our proposed scheme, low-resolution information is transmitted using Grassmannian constellations discussed earlier, while high-resolution information is encoded in the indices of the transmitter antennas active during the signaling interval. We will show later that the noncoherent detector performance is not affected by

the incremental HR information encoded in the antenna indices.

3.1 Brief Overview of Spatial Modulation

The idea of encoding information in the indices of used transmit antennas was first proposed by Mesleh et al. [37]. It was seen as an effort to eliminate two common problems in conventional MIMO systems; *inter-channel interference* (ICI) which required complex decoding algorithms, and the need for precise synchronization between antenna (*Inter-antenna synchronization* (IAS)). By activating only one antenna in each channel use both problems can be eliminated. The original concept is depicted in figure 3.1. Suppose you need to send

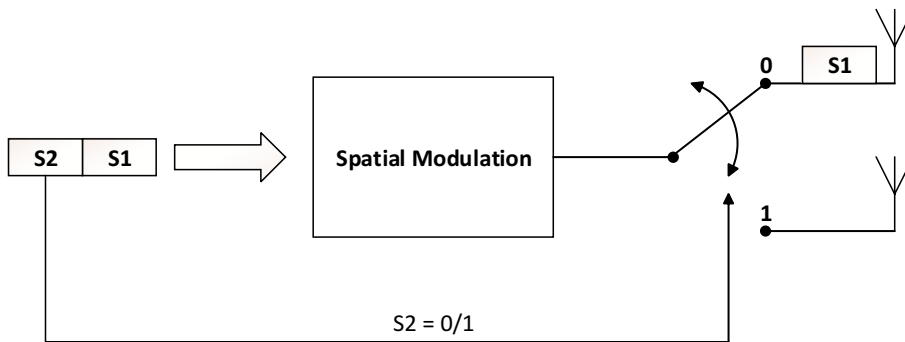


FIGURE 3.1: Illustration of the basic concept of Spatial Modulation

two APM symbols s_1 and s_2 , you can transmit only one symbol s_1 explicitly, while the other symbol is implicitly transmitted by the choice of the index of the transmitter antenna used.

Later Jedadeyban et al. [27] proposed to get rid of the APM symbols, and encode the information only in the active antenna index, this scheme was called *space shift keying* (SSK). Then, the concept was generalized to what is called *generalized space shift keying* [26]. In GSSK, each sequence of bits $\mathbf{b} = [b_1 b_2 \dots b_n]$ is mapped to a constellation vector $\mathbf{x} = [x_1 x_2 \dots x_M]$, where M is the number of available

transmitter antenna. At any signaling interval, only M_A transmitter antennas are active; hence, the vector \mathbf{x} has only M_A nonzero values, and number of possible antenna combinations is given by $\binom{M}{M_A}$, each antenna combination represent a possible codeword. In Fig. 3.2, the performance of GSSK for different M and M_A is plotted against V-BLAST [11] and SM [25]. All simulated schemes have a spectral efficiency $m = 3$ bits/s/Hz, and the number of receiver antennas is $N = 4$.

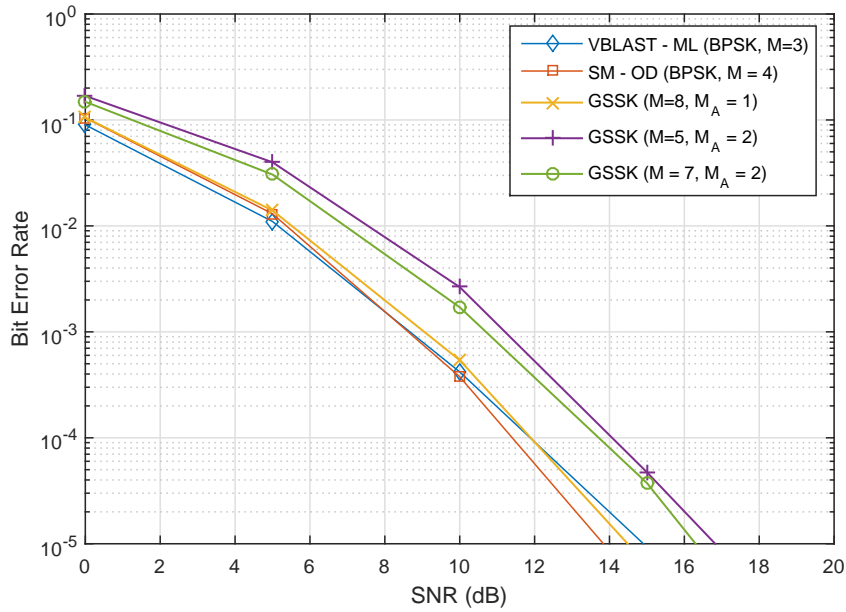


FIGURE 3.2: BER performance of GSSK versus V-BLAST, and SM, for = 3 blts/s/Hz transmission ($N = 4$).

In subsequent sections, we combine both Grassmannian constellations and GSSK to design a multilayer encoding scheme for the MIMO multicast channel.

3.2 System Model

A MIMO multicast system is considered. The transmitter has M antennas of which only M_A are active at any time, and the i -th receiver has N_i antennas. The channel is assumed to be a quasi-static Rayleigh flat fading MIMO channel, and the noise is additive white Gaussian noise. The system can be modeled as:

$$\begin{aligned} \mathbf{Y}_i &= \mathbf{S}\mathbf{H}_i + \sqrt{\frac{M_A}{\rho T}}\mathbf{W}_i \\ &= \mathbf{U}\mathbf{A}\mathbf{H}_i + \sqrt{\frac{M_A}{\rho T}}\mathbf{W}_i, \quad i \in \mathcal{N}_C \cup \mathcal{N}_{NC} \end{aligned} \tag{3.1}$$

where \mathbf{Y}_i is the $T \times N_i$ received matrix at the i -th receiver. $\mathbf{S} = \mathbf{U}\mathbf{A}$ is the $T \times M$ transmitted matrix, where \mathbf{U} is the $T \times M_A$ matrix containing the LR information and \mathbf{A} is the $M_A \times M$ antenna selection matrix containing the HR information. \mathbf{H}_i denote the $M \times N_i$ channel matrix between the transmitter and the i -th receiver and \mathbf{W}_i denote the $T \times N_i$ noise matrix at the i -th receiver. \mathcal{N}_C and \mathcal{N}_{NC} denote the set of coherent and non-coherent receivers, respectively. The entries of the channel and noise matrices are independent, and identically distributed, circularly symmetric, complex Gaussian random variables with zero means and unit variances $\mathcal{CN}(0, 1)$. The channel matrix entries are assumed to remain constant for the signaling period T , and then change independently to a new realization. Throughout the rest of the chapter, receiver index i is dropped for notational convenience.

There are two classes of receivers. The first class of receivers are assumed to have perfect knowledge of channel coefficients (CSI), and thus able to perform coherent detection to retrieve both the LR information encoded in \mathbf{U} , and the incremental HR information encoded

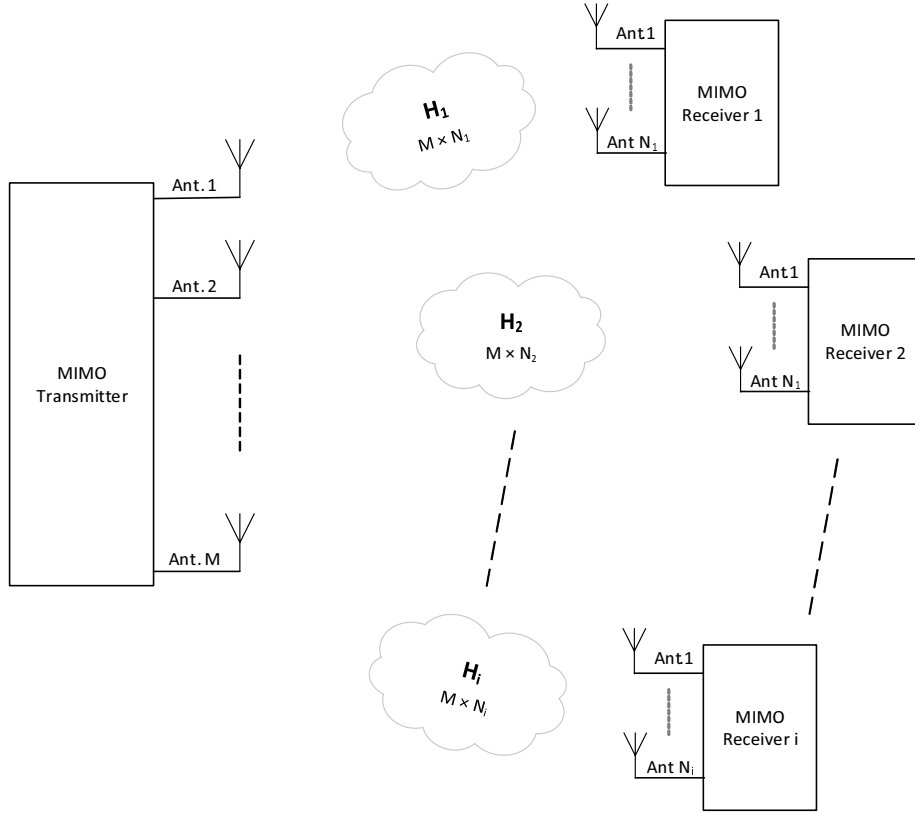


FIGURE 3.3: The MIMO Multicast System Model

in \mathbf{A} . The second class of receivers do not have knowledge of the channel coefficients, and thus perform non-coherent detection to retrieve only the LR information in \mathbf{U} .

The LR information is encoded in the subspace spanned by the matrix \mathbf{U} which represent a single point on the Grassmann manifold, whereas the incremental HR information is encoded implicitly in the choice of the indices of the M_A active antennas used to transmit the matrix \mathbf{U} using GSSK. The rows of the antenna selection matrix \mathbf{A} are standard unit vectors (\mathbf{e}_i) multiplied by $e^{j\theta_i}$, specifying which antennas are active during the signaling period T and ensuring maximum separation between transmitted matrices. The construction of the matrices \mathbf{U} , \mathbf{A} and the role of $e^{j\theta_i}$ will be discussed further in section 3.3.

3.3 Code Structure

In the proposed scheme, information is encoded in both points on the Grassmann manifold and the indices of the used transmitter's antennas. The transmitted matrix \mathbf{X} is the product of two matrices. The matrix \mathbf{U} represents points on the Grassmann manifold and contains the LR information which is detected by both classes of receivers, and the antenna selection matrix \mathbf{A} contains the incremental HR information which is only detected by receivers that have CSI. The construction of both matrices are discussed next. Throughout the rest of the chapter, $|\mathcal{C}_L|$ and $|\mathcal{C}_H|$ denote the cardinalities of the LR and HR constellations, respectively.

3.3.1 LR Layer (Non-coherent) Code Construction

To achieve the capacity of the non-coherent layer at high SNR, the matrix \mathbf{U} should represent isotropically distributed M_A -dimensional subspaces of \mathbb{C}^T , provided that $N_i \geq M_A$, $T \geq N_i + M_A$ and $M_A \leq \lfloor T/2 \rfloor$. These conditions are necessary to ensure that the noncoherent code can achieve the capacity [49] and are assumed to be satisfied throughout. Each subspace represent a single point on the compact Grassmann manifold. As discussed earlier in chapter 2, it was shown in [15], that the chordal Frobenius norm is an appropriate metric to measure the distance between Grassmannian constellation points. The chordal Frobenius norm between any pair of matrices \mathbf{U}_i and \mathbf{U}_j is given by $\sqrt{2M_A - 2\text{Tr}(\boldsymbol{\Sigma}_{ij})}$, where $\boldsymbol{\Sigma}_{ij}$ is the matrix containing the singular values of the matrix $\mathbf{U}_i^\dagger \mathbf{U}_j$ [2]. The Grassmannian constellation points are designed simultaneously using the direct method in [15]. The $|\mathcal{C}_L|$ -point constellation design problem is

equivalent to the optimization problem given by:

$$\begin{aligned} & \min_{\{\mathbf{U}_k\}_{k=1}^{|\mathcal{C}_L|}} \max_{1 \leq i, j \leq |\mathcal{C}_L|} \text{Tr}(\boldsymbol{\Sigma}_{ij}) \\ & \text{subject to } \mathbf{U}_k \in \mathbb{G}_{M_A} \mathbb{C}^T, \quad k = 1, 2, \dots, |\mathcal{C}_L|. \end{aligned} \quad (3.2)$$

We already addressed the solution of this optimization problem in Chapter 2 and Appendix A.

3.3.2 HR Layer (coherent) Code Construction

The incremental HR information is encoded in the indices of the active antennas during the signaling interval, and is represented by the antenna selection matrix \mathbf{A} . This matrix specifies the indices of the M_A active antennas used to transmit the matrix \mathbf{U} . Let \mathbf{e}_m denote the standard unit vector of size $1 \times M$ whose elements are all zeros except the m -th element which is equal to one. Each row of \mathbf{A} is a standard unit vector multiplied by a complex exponential $e^{j\theta}$. In particular, each realization of \mathbf{A} will take the form

$$\mathbf{A} = \begin{bmatrix} \mathbf{e}_x e^{j\theta_1} \\ \mathbf{e}_y e^{j\theta_2} \\ \vdots \\ \mathbf{e}_z e^{j\theta_{M_A}} \end{bmatrix}, \quad (3.3)$$

where

$$\mathbf{e}_1 = \begin{bmatrix} 1 \\ 0 \\ 0 \\ \vdots \\ 0 \end{bmatrix}^T, \quad \mathbf{e}_2 = \begin{bmatrix} 0 \\ 1 \\ 0 \\ \vdots \\ 0 \end{bmatrix}^T, \quad \dots, \quad \mathbf{e}_M = \begin{bmatrix} 0 \\ 0 \\ \vdots \\ 0 \\ 1 \end{bmatrix}^T, \quad (3.4)$$

and the rotation angles $\theta_1, \theta_2, \dots, \theta_{M_A}$ are chosen by computer numerical search, for a particular Grassmannian constellation, to ensure maximum possible diversity and maximum distance between the codewords of the resulting space time block code. If the rotation angles are not used, the diversity order will decrease. Each row of the antenna selection matrix \mathbf{A} represents the selection of one antenna element out the available M antennas at the transmitter, and each realization of \mathbf{A} represents a particular combination of transmit antennas out of the possible $\binom{M}{M_A}$ combinations. The following simple example illustrates how the HR layer data is encoded.

Example 1 ($M = T = 4, M_A = 2$ and $|\mathcal{C}_H| = 4$): In this example the LR matrix $\mathbf{U} = [\mathbf{u}_1 \ \mathbf{u}_2]$ belongs to the Grassmannian constellation with cardinality $|\mathcal{C}_L|$ and represents $\log_2 |\mathcal{C}_L|$ information bits, and the matrix \mathbf{A} represents the HR information and has four different realizations that represent 4 different combinations of antennas indices (out of the possible $\binom{4}{2} = 6$). This HR layer code convey 2 information bits per signaling interval T . For any realization of the LR matrix \mathbf{U} , the HR matrix \mathbf{A} can take one of four possible realizations depending on the 2 HR information bits. So, for a specific LR matrix \mathbf{U} , the transmitted matrix \mathbf{S} can be one of these four codewords:

$$\begin{aligned}
\mathbf{C}_{11} &= \mathbf{U}\mathbf{A}_{11} = \begin{pmatrix} \mathbf{U} & \mathbf{0}_{4 \times 2} \end{pmatrix} \\
\mathbf{C}_{12} &= \mathbf{U}\mathbf{A}_{12} = \begin{pmatrix} \mathbf{0}_{4 \times 2} & \mathbf{U} \end{pmatrix} \\
\mathbf{C}_{21} &= \mathbf{U}\mathbf{A}_{21} = \begin{pmatrix} \mathbf{0}_{4 \times 1} & \mathbf{u}_1 e^{j\theta_1} & \mathbf{u}_2 e^{j\theta_2} & \mathbf{0}_{4 \times 1} \end{pmatrix} \\
\mathbf{C}_{22} &= \mathbf{U}\mathbf{A}_{22} = \begin{pmatrix} \mathbf{u}_1 e^{j\theta_3} & \mathbf{0}_{4 \times 2} & \mathbf{u}_2 e^{j\theta_4} \end{pmatrix}
\end{aligned} \tag{3.5}$$

. Define a group of non-interfering codewords with b elements as a group of codewords that have non-overlapping columns such that

$\mathbf{C}_{ij}\mathbf{C}_{ik}^H = \mathbf{0}_{T \times T}$, $j, k = 1, 2, \dots, b$, $j \neq k$. Hence, the four codewords in this example constitute two non-interfering codewords groups;

$$\begin{aligned} \mathcal{C}_1 &= \{\mathbf{C}_{11}, \mathbf{C}_{12}\} \\ \mathcal{C}_2 &= \{\mathbf{C}_{21}, \mathbf{C}_{22}\} \end{aligned} \quad (3.6)$$

and the complete code is $\bigcup_{i=1}^2 \mathcal{C}_i$. The rotation angles are optimized using numerical search for a given Grassmanian constellation to maximize the minimum distance between codewords, and ensure maximum diversity order is achieved. Throughout this chapter, we use the Frobenius norm of the difference matrix between any two codewords denoted by $\|\mathbf{C}_i - \mathbf{C}_j\|_F$ as a measure of distance between those two codewords. Maximizing the minimum distance $\|\mathbf{C}_i - \mathbf{C}_j\|_F$ between all possible codewords is called the trace criterion for design of space time codes [23] [24]. Define the minimum distance between two non-interfering groups \mathcal{C}_i and \mathcal{C}_j as

$$d_{\min}(\mathcal{C}_i, \mathcal{C}_j) = \min_{k,l} \|\mathbf{C}_{ik} - \mathbf{C}_{jl}\|_F, \quad (3.7)$$

and the minimum distance of the entire codebook $\bigcup_{\forall i} \mathcal{C}_i$ as:

$$d_{\min}(\mathcal{C}) = \min_{i,j,i \neq j} d_{\min}(\mathcal{C}_i, \mathcal{C}_j). \quad (3.8)$$

Using the scheme illustrated in the example, we can send two extra HR information bits per signaling interval T . In general, for arbitrary number of transmit antennas M and number of active antennas M_A , a technique similar to that described in [9] can be used. This technique is given as follows:

1. Given the total number of transmit antennas M and the number of active antennas M_A , calculate cardinality of the HR constellation $|\mathcal{C}_H|$ as the largest integer $\leq \binom{M}{M_A}$ that is a power of 2.
2. Calculate the number of codewords in each non-interfering group of codewords as $b = \lfloor \frac{M}{M_A} \rfloor$, and the total number of non-interfering groups as $n = \lceil \frac{|\mathcal{C}_H|}{b} \rceil$. In general, the last non-interfering codewords group does not need to have b codewords.
3. Construct the first non-interfering group \mathcal{C}_1 as:

$$\begin{aligned} \mathcal{C}_1 = \{ & (\mathbf{U} \quad \mathbf{0}_{T \times (M-M_A)}), \\ & (\mathbf{0}_{T \times M_A} \quad \mathbf{U} \quad \mathbf{0}_{T \times (M-2M_A)}), \\ & (\mathbf{0}_{T \times 2M_A} \quad \mathbf{U} \quad \mathbf{0}_{T \times (M-3M_A)}), \quad \cdot \quad (3.9) \\ & \vdots \\ & (\mathbf{0}_{T \times (b-1)M_A} \quad \mathbf{U} \quad \mathbf{0}_{T \times (M-bM_A)}) \} \end{aligned}$$

4. Construct the remaining non-interfering groups $\mathcal{C}_i, i = 1, 2, \dots, n$ sequentially as in step 3 while making sure that
 - Every group contains codewords that have non-overlapping columns.
 - The same antenna combination can never be used more than once.
5. Finally, the rotation angles are chosen by numerical search to maximize the minimum distance between codewords for a given Grassmannian constellation. In particular $\theta_{opt} = \arg \max_{\theta} d_{min}(\mathcal{C})$, where θ is a vector comprising all the rotation angles.

The spectral efficiency of the proposed scheme can be easily estimated to be $\eta = \frac{1}{T} (\log_2 |\mathcal{C}_H| + \log_2 |\mathcal{C}_L|)$ bits/s/Hz. It is worth mentioning that as long as this technique is used, different choices of antenna combinations in non-interfering groups will exhibit the same performance for uncorrelated channels.

3.4 Detectors

In this section, three types of detectors are discussed. For the class of receivers that do not have reliable CSI, the optimal non-coherent detector is introduced. For the class of receivers that possess reliable CSI, two detectors are introduced. The optimal ML coherent receiver jointly detects the LR information and the incremental HR information but is computationally expensive. To reduce detection complexity, a sub-optimal two step detector may be used to first detect the LR information, and then detect the HR information.

3.4.1 The Optimal Non-coherent Detector

The optimal ML detector when the channel is unknown to the receiver, but the channel coefficients are i.i.d complex Gaussian random variables, is given by

$$\hat{\mathbf{U}} = \arg \max_{\mathbf{U}} \frac{\exp \left(- \text{Tr} \left(\mathbf{Y}^\dagger \left(\frac{M_A}{\rho T} \mathbf{I}_T + \mathbf{U}\mathbf{U}^\dagger \right)^{-1} \mathbf{Y} \right) \right)}{\pi^{TN} \det^N \left(\frac{M_A}{\rho T} \mathbf{I}_T + \mathbf{U}\mathbf{U}^\dagger \right)}. \quad (3.10)$$

However, since the matrix \mathbf{U} is unitary the ML detector can be simplified to

$$\hat{\mathbf{U}} = \arg \max_{\mathbf{U}} \text{Tr}(\mathbf{Y}^\dagger \mathbf{U}\mathbf{U}^\dagger \mathbf{Y}), \quad (3.11)$$

which is equivalent to the GLRT receiver given by [5]

$$\hat{\mathbf{U}} = \arg \max_{\mathbf{U}} \sup_{\mathbf{H}} p(\mathbf{Y}|\mathbf{U}, \mathbf{H}). \quad (3.12)$$

For the optimality of the detector in (3.11) to hold, the unitary LR matrix \mathbf{U} has to be subjected to a channel matrix whose entries are i.i.d complex Gaussian random variables. From (3.1), the equivalent channel matrix "seen" by the non-coherent layer is $\mathbf{H}_{eq} = \mathbf{A}\mathbf{H}_i$. The matrix \mathbf{A} merely picks the rows corresponding to the active transmit antennas and rotate them. Since all the entries of \mathbf{H} are circularly symmetric, rotation does not alter the distribution of the channel coefficients, and the performance of the non-coherent detector is unaffected by the incremental HR information encoded in \mathbf{A} .

3.4.2 Optimal (Joint) One Step Coherent Detector

The optimal detector in AWGN when the channel matrix \mathbf{H} is known at the receiver, is the minimum distance detector given by:

$$\hat{\mathbf{S}} = \arg \min_{\mathbf{S}} \|\mathbf{Y} - \mathbf{S}\mathbf{H}\|_F^2 \quad (3.13)$$

The detector in (3.13) requires an exhaustive search over all possible values of \mathbf{S} . Denote the cardinality of Grassmannian LR constellation by $|\mathcal{C}_L|$, and the cardinality of the HR spatial constellation by $|\mathcal{C}_H|$. Hence, the detector requires $|\mathcal{C}_L| |\mathcal{C}_H|$ metric computations. For large constellations this would be prohibitively expensive computationally and the two step detector proposed in the next subsection is a more practical option.

3.4.3 Two Step Suboptimal Coherent Detector

To reduce the complexity of detection, the two step detector detects the LR information and then detects the incremental HR information. In the first step, the optimal non-coherent approach in (3.11) is used to detect the Grassmannian codeword in matrix \mathbf{U} . The detected matrix $\hat{\mathbf{U}}$ is assumed to be correct, and is fed to the second step. In the second step, a maximum likelihood detector is used to detect \mathbf{A} :

$$\hat{\mathbf{A}} = \arg \min_{\mathbf{A}} \|\mathbf{Y} - \hat{\mathbf{U}}\mathbf{A}\mathbf{H}\|_F^2 \quad (3.14)$$

The two step detector requires only $|\mathcal{C}_L| + |\mathcal{C}_H|$ metric computations, which is significantly more efficient than the $|\mathcal{C}_L| |\mathcal{C}_H|$ metric computations required by the optimal joint detector. However, the GLRT used in the first step does not take advantage of the CSI available; therefore, there is a performance degradation compared to the optimal joint detector.

3.5 Simulation Results

In this section, some simulation results for the proposed system is presented. In all simulations, $M_A = N = 2$ and $M = T = 4$, and the 4-point HR layer code presented earlier in Example 1 is used. Figure 3.4 shows the block error probability of the LR layer using the non-coherent detector. As expected, antenna selection and rotation performed by the HR matrix \mathbf{A} has no effect on the performance of the non-coherent receiver, this is also observed in figure 3.7.

In Figure 3.5, the gain of the rotation is not obvious in the 2-step detector. This is because the size of the LR constellation is much

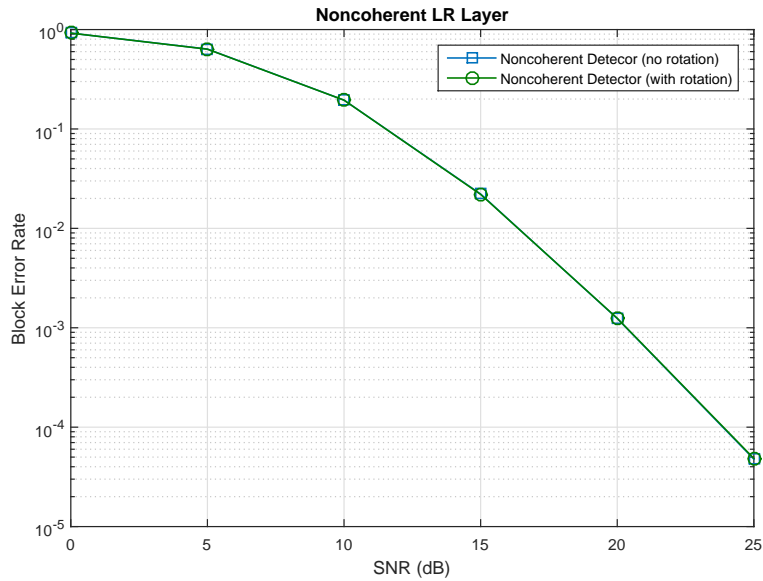


FIGURE 3.4: Performance of the noncoherent detector. (256 point LR constellation constructed on $\mathbb{G}_{4,2}$ using the direct method)

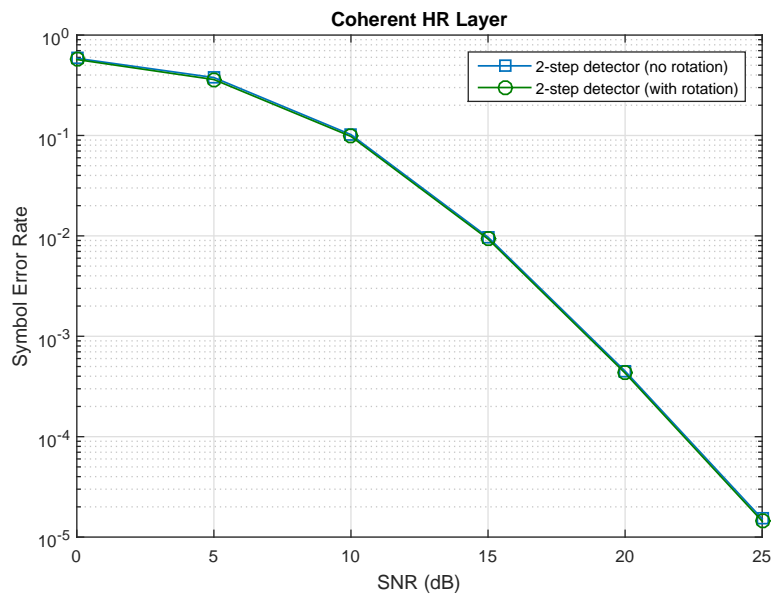


FIGURE 3.5: Performance of the 2-step coherent detector. (256 point LR constellation constructed on $\mathbb{G}_{4,2}$ using the direct method and 4 point HR spatial constellation.)

larger than the spatial HR constellation, and most errors occur because the first step fed an incorrect $\hat{\mathbf{U}}$ to the second step. Therefore increasing the distance between spatial constellation points will not have a significant effect on the HR layer performance.

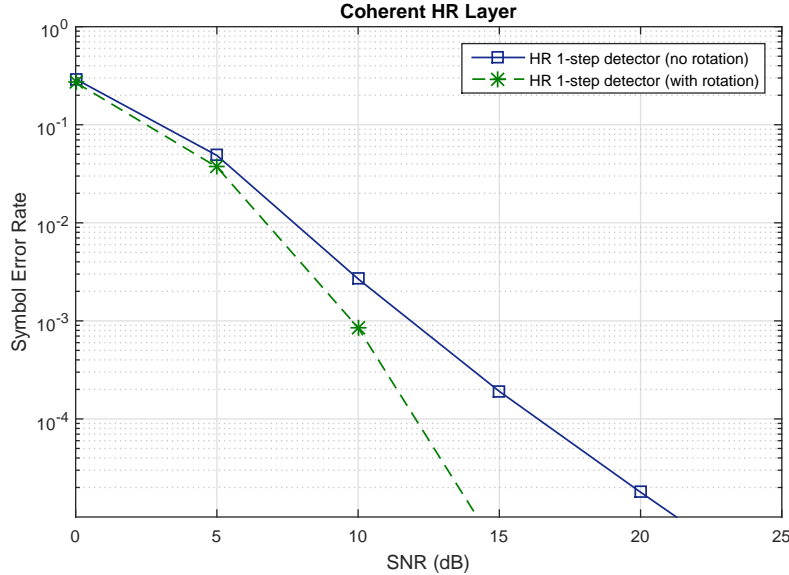


FIGURE 3.6: Performance of the 1-step coherent detector. (256 point LR constellation constructed on $\mathbb{G}_{4,2}$ using the direct method and 4 point HR spatial constellation.)

However, from Figure 3.6, it is obvious that the optimized rotation angles in \mathbf{A} achieve significant gain in the performance of the joint 1-step detector.

To observe the effect of optimized rotation angles on the performance of the two step detector, the constellation size of the LR layer was reduced to only two. Figure 3.8 shows the performance of the two step detector in that case. The vital role of the rotation angles is evident, and a gain of almost 7 dB can be observed at a symbol error rate of 10^{-4} .

Finally, in Fig. 3.9, we compare the performance of our proposed HR layer code against the HR layer code proposed in [21]. In [21], the same system model used here applies, and the LR layer information

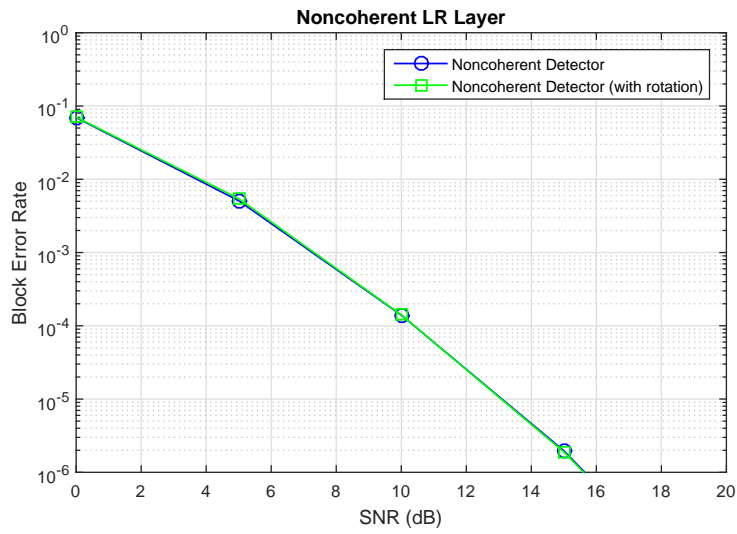


FIGURE 3.7: Performance of the noncoherent detector. (2 point LR constellation constructed on $\mathbb{G}_{4,2}$).

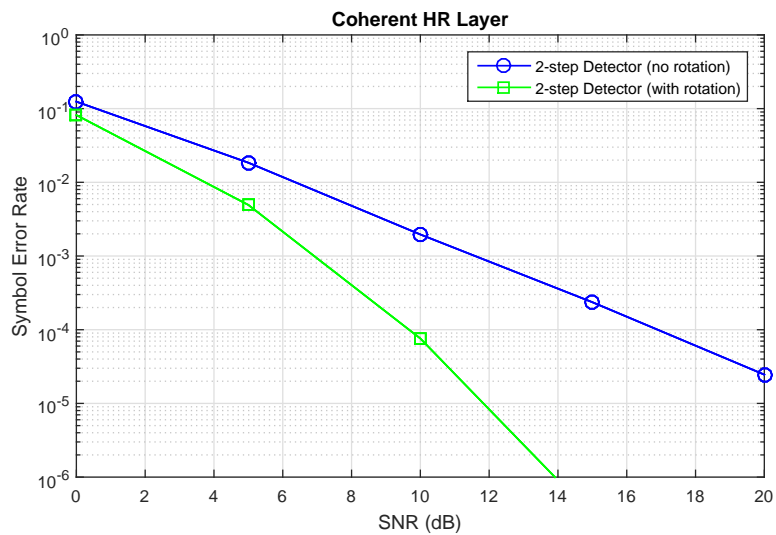


FIGURE 3.8: Performance of the 2-step coherent detector. (2 point LR constellation constructed on $\mathbb{G}_{4,2}$ and 4 point HR spatial constellation.)

is also encoded the subspace spanned by the transmitted codeword, but the HR layer information is encoded in the particular basis of the subspace. Square unitary matrices are used to rotate the subspace basis, and are designed by direct optimization on the unitary group \mathbb{U}_M . Results show that in the simulated case, the proposed spatial codes outperforms the codes in [21], and consequently [20].

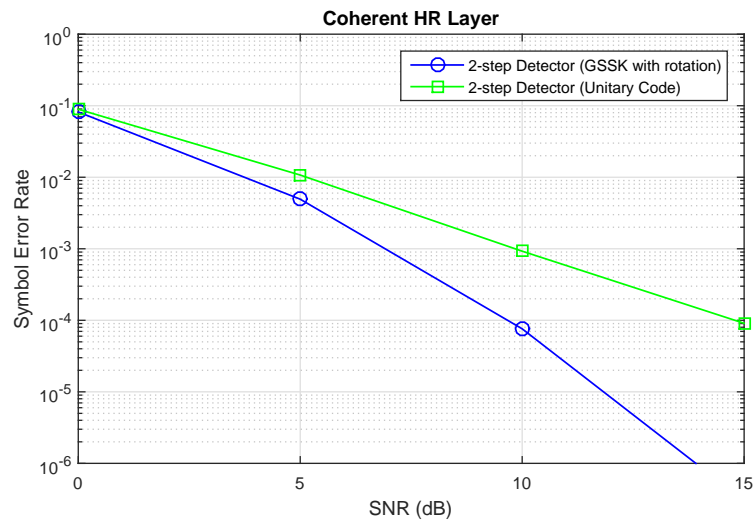


FIGURE 3.9: Comparison with the unitary code in [21] (2 point LR constellation constructed on $\mathbb{G}_{4,2}$ and 4 point HR constellations.)

Chapter 4

Conclusions and Future Work

4.1 Conclusions

This thesis consisted of two parts. In chapter 3, we proposed a new design approach to construct space-time codes for the non-coherent MIMO channel. In our approach, we let the number of transmit antennas vary across constellation points. We used a conjugate gradient method to design Grassmannian constellations of different dimensions, and mixed points from these constellations to construct new constellations where the number of transmit antennas used is variable. Numerical simulations were used to evaluate the performance of the proposed constellations, and results show that our constellations show superior performance at low-to-moderate SNRs, without sacrificing performance at practical higher SNRs up to 25 dB.

In chapter 4, we proposed a new multi-resolution space-time signaling scheme for the MIMO multicast channel. The proposed scheme encodes information in two layers; low-resolution information is encoded using a Grassmannian noncoherent code that could be decoded without knowledge of CSI at the receiver, while high-resolution incremental information is encoded in the indices of the transmitter antennas using GSSK. We showed that the HR layer is transparent to

the underlying LR layer. Numerical simulations suggest that the error performance of the HR layer in the proposed scheme is superior to schemes using conventional unitary space-time block codes [20], and unitary constellations generated by direct numerical optimization on the unitary group [21].

4.2 Future Work

We mention two directions to expand the work presented in this thesis. For the first part on noncoherent MIMO codes, the most important contribution to make would be to find the ergodic capacity for any SNR, and thus find the optimal signaling distribution that would achieve capacity regardless of the SNR.

For the second part on multilayer coding, one possible direction for expanding the work done would be to explore using unitary space-time on top of transmitting antennas indices to encode information in the high-resolution layer. Using unitary codes for the high-resolution layer was proposed in [19] [20], but encoding additional information in the indices of the transmitting antennas would boost the transmitted data rates in the high-resolution layer.

Appendix A

Conjugate Gradient on The Grassmann Manifold

Nonlinear conjugate gradient techniques are simple to implement, require little storage, and have superlinear convergence in the limit. Conjugate gradient method was first developed to solve a linear system of n equations in n unknowns, or equivalently, minimize a quadratic function on Euclidean space \mathcal{R}^n in n steps[33]. However, it could be easily modified to find the minimum of a nonquadratic function on \mathcal{R}^n . In particular, algorithms by Fletcher-Reeves [10] and Polak-Ribiere [40] assume that the second order Taylor expansion provides a sufficiently accurate representation of the function near the minimum, and thus general functions can be minimized using the conjugate gradient algorithm; but, convergence in n steps is not guaranteed.

In Euclidean space, the conjugate gradient method is straight forward. Given a function $f : \mathcal{R}^n \mapsto \mathcal{R}$ with local minimum at \hat{x} which is at least twice differentiable and an initial point $x_0 \in \mathcal{R}^N$, compute the negative gradient direction $H_0 = -G_0$; then, the iterative part starts. In the iterative part, (i) a line search is performed to find the step size t_{min} which minimizes $f(x_{k+1})$ where $x_{k+1} = x_k + tH_k$, (ii)

the point is updated $x_{k+1} = x_k + t_{min}H_k$, (iii) the gradient at the updated point G_{k+1} is computed and (iv) the new search direction is computed $H_{k+1} = -G_{k+1} + \gamma_k H_k$, where γ_k is chosen to ensure conjugacy between old and new search directions [13]. It is worth mentioning that when the objective function is non quadratic, but closely approximated by a quadratic function, the algorithm converges more rapidly if it is reset by setting $H_{k+1} = G_{k+1}$ every n step.

Algorithm 2 Conjugate Gradient for Minimizing $F(Y)$ on The Grassmann Manifold

Input: Initial point on the Grassmann manifold Y_0 .

Output: Another point on the Grassmann manifold that minimizes the objective function $F(Y)$

- 1: Compute $G_0 = F_{Y_0} - Y_0 Y_0^\dagger F_{Y_0}$ then set $H_0 = -G_0$.
- 2: **while** true **do**
- 3: Call a line search over t to minimize $F(Y_k(t))$ where

$$Y(t) = YV \cos(\Sigma t)V^\dagger + U \sin(\Sigma t)V^\dagger$$

and $U\Sigma V^\dagger$ is the compact singular value decomposition of H_k .

- 4: Update: $t_k = t_{min}$ and $Y_{k+1} = Y_k(t_k)$.
- 5: Compute $G_{k+1} = F_{Y_{k+1}} - Y_{k+1} Y_{k+1}^\dagger F_{Y_{k+1}}$
- 6: Parallel transport H_k and G_k to the point Y_{k+1} :

$$\begin{aligned} \tau H_k &= (-Y_k V \sin(\Sigma t_k) + U \cos(\Sigma t_k)) \Sigma V^\dagger \\ \tau G_k &= G_k - (-Y_k V \sin(\Sigma t_k) + U (I - \cos(\Sigma t_k))) U^\dagger G_k \end{aligned}$$

- 7: Compute new search direction: $H_{k+1} = -G_{k+1} + \gamma_k \tau H_k$, where $\gamma_k = \frac{\langle G_{k+1} - \tau G_k, G_{k+1} \rangle}{\langle G_k, G_k \rangle}$ (Polak-Ribiere), and $\langle \Delta_1, \Delta_2 \rangle = \text{Tr} \Delta_1^\dagger \Delta_2$
 - 8: Reset $H_{k+1} = -G_{k+1}$ if $k + 1 \equiv 0 \pmod{M(T - M)}$.
 - 9: Stopping check:
 - 10: **if** $F(Y_k) - F(Y_{k+1}) \leq \epsilon$ **then**
 - 11: stop
 - 12: **end if**
 - 13: **end while**
-

The ideas behind the conjugate gradient algorithm in flat space can be generalized to Riemannian geometry. However, unlike flat

space, the line search will be performed along a geodesic on the manifold and tangent vectors must be parallel transported along geodesics to compute the new search direction. Let \mathbb{G} be a smooth Grassmannian manifold, and let f be a smooth differentiable function defined on this manifold. Given an initial point Y_0 on \mathbb{G} , compute gradient of F at Y_0 given by G_0 and set search direction $H_0 = -G_0$. The iterative part goes as follows: (i) perform a line search over t to find the step size t_{min} that minimizes $F(Y(t))$ along the geodesic in the search direction H_k , (ii) update $t_k = t_{min}$ and $Y_{k+1} = Y_k(t_k)$, (iii) compute the gradient at Y_{k+1} given by G_{k+1} , (iv) parallel transport the tangent vector G_k and H_k to the updated point Y_{k+1} and (v) compute the new search direction combining the old search direction and the old gradient. The new and old search directions must satisfy the conjugacy condition. To improve the computational efficiency of this step, finite difference approximations are usually used as in the formulas proposed by Fletcher-Reeves [10] and Polak-Ribiere [40]. Using the ideas and concepts discussed earlier, the conjugate gradient algorithm to minimize a function defined on the Grassmann manifold is given in Algorithm 2.

Bibliography

- [1] M. J. Borran, A. Sabharwal, and B. Aazhang. “On Design Criteria and Construction of Noncoherent Space–Time Constellations”. In: *IEEE Trans. Info. Theory* 49.10 (Oct. 2003), pp. 2332–2351.
- [2] A. Edelman, T. Arias, and S. Smith. “The geometry of algorithms with orthogonality constraints”. In: *SIAM J. Matrix Anal. Appl.* 14.2 (1998), pp. 303–353.
- [3] S. M. Alamouti. “A simple transmit diversity technique for wireless communications”. In: *IEEE Journal on Selected Areas in Communications* 16.8 (Oct. 1998), pp. 1451–1458. ISSN: 0733-8716. DOI: [10.1109/49.730453](https://doi.org/10.1109/49.730453).
- [4] Arogyaswami Paulraj, Rohit Nabar, and Dhananjay Gore. *Introduction to Space-Time Wireless Communications*. 1st. New York, NY, USA: Cambridge University Press, 2008. ISBN: 0-521-06593-3, 978-0-521-06593-1.
- [5] M. Brehler and M. K. Varanasi. “Asymptotic Error Probability Analysis of Quadratic Receivers in Rayleigh-Fading Channels With Applications to a Unified Analysis of Coherent and Noncoherent Space-Time Receivers”. In: *IEEE Trans. Info. Theory* 47.6 (Sept. 2001), pp. 2383–2399.
- [6] D. Argawal, T. Richardson, and R. Urbanke. “Multiple-antenna Signal Constellations for Fading Channels”. In: *IEEE Trans. Info. Theory* 47.6 (Sept. 2001), pp. 2618–2626.

- [7] David Tse and Pramod Viswanath. *Fundamentals of Wireless Communication*. Cambridge University Press, July 2005. ISBN: 978-0-521-84527-4.
- [8] Pranav Dayal, Matthias Brehler, and Mahesh K. Varanasi. “Leveraging coherent space-time codes for noncoherent communication via training”. In: *IEEE TRANS. INFORM. THEORY* 50.9 (2004), pp. 2058–2080.
- [9] E. Basar, U. Aygolu, E. Panayirci, and H. Poor. “Space-Time Block Coded Spatial Modulation”. In: *IEEE Trans. Comm.* 59.3 (Mar. 2011), pp. 823–823.
- [10] R. Fletcher and C. M. Reeves. “Function minimization by conjugate gradients”. en. In: *The Computer Journal* 7.2 (Jan. 1964), pp. 149–154. ISSN: 0010-4620, 1460-2067. DOI: [10.1093/comjnl/7.2.149](https://doi.org/10.1093/comjnl/7.2.149). URL: <http://comjnl.oxfordjournals.org/content/7/2/149> (visited on 12/01/2016).
- [11] G. J. Foschini. “Layered space-time architecture for wireless communication in a fading environment when using multi-element antennas”. In: *Bell Labs Technical Journal* 1.2 (1996), pp. 41–59. ISSN: 1089-7089. DOI: [10.1002/bltj.2015](https://doi.org/10.1002/bltj.2015).
- [12] G. J. Foschini and M. J. Gans. “On limits of wireless communications in a fading environment when using multiple antennas”. In: *Wireless Personal Communications* 6 (1998), pp. 311–335.
- [13] G. H. Golub and C. F. Van Loan. *Matrix Computations*. 3rd ed. Baltimore, MD: The Johns Hopkins University Press, 1996.
- [14] H. El Gamal, D. Aktas, and M. O. Damen. “Noncoherent space-time coding: An algebraic perspective”. In: *IEEE Transactions on Information Theory* 51.7 (July 2005), pp. 2380–2390. ISSN: 0018-9448. DOI: [10.1109/TIT.2005.850139](https://doi.org/10.1109/TIT.2005.850139).

-
- [15] R. H. Gohary and T. N. Davidson. "Noncoherent MIMO Communication: Grassmannian Constellations and Efficient Detection". In: *IEEE Trans. Info. Theory* 55.3 (Mar. 2009), pp. 1176–1205.
- [16] A. Goldsmith et al. "Capacity limits of MIMO channels". In: *IEEE Journal on Selected Areas in Communications* 21.5 (June 2003), pp. 684–702. ISSN: 0733-8716. DOI: [10.1109/JSAC.2003.810294](https://doi.org/10.1109/JSAC.2003.810294).
- [17] Babak Hassibi and Bertrand Hochwald. "How Much Training is Needed in Multiple-Antenna Wireless Links?" In: *IEEE Trans. Inform. Theory* 49 (2000), pp. 951–963.
- [18] B. M. Hochwald et al. "Systematic design of unitary space-time constellations". In: *IEEE Transactions on Information Theory* 46.6 (Sept. 2000), pp. 1962–1973. ISSN: 0018-9448. DOI: [10.1109/18.868472](https://doi.org/10.1109/18.868472).
- [19] M. T. Hussien et al. "Layered coding with non-coherent and coherent layers over fading channels". In: *2014 12th International Symposium on Modeling and Optimization in Mobile, Ad Hoc, and Wireless Networks (WiOpt)*. May 2014, pp. 203–209. DOI: [10.1109/WIOPT.2014.6850300](https://doi.org/10.1109/WIOPT.2014.6850300).
- [20] Mohammad T. Hussien et al. "Multi-resolution broadcasting over the Grassmann and Stiefel manifolds". In: *2014 IEEE International Symposium on Information Theory (2014)*. DOI: [10.1109/isit.2014.6875165](https://doi.org/10.1109/isit.2014.6875165).
- [21] Mohammad T. Hussien et al. "Space-Time Block Codes over the Stiefel Manifold". In: *2015 IEEE Global Communications Conference (GLOBECOM) (2015)*. DOI: [10.1109/glocom.2015.7417496](https://doi.org/10.1109/glocom.2015.7417496).

-
- [22] I. Kammoun, A. M. Cipriano, and J. C. Belfiore. "Non-Coherent Codes over the Grassmannian". In: *IEEE Trans. Wireless Communications* 6.10 (Oct. 2007), pp. 2332–2351.
- [23] D. M. Ionescu. "New results on space-time code design criteria". In: *WCNC. 1999 IEEE Wireless Communications and Networking Conference (Cat. No.99TH8466)*. 1999, 684–687 vol.2. DOI: [10.1109/WCNC.1999.796731](https://doi.org/10.1109/WCNC.1999.796731).
- [24] Hamid Jafarkhani. *Space-Time Coding: Theory and Practice*. English. 1 edition. Cambridge, UK ; New York: Cambridge University Press, Oct. 2005. ISBN: 978-0-521-84291-4.
- [25] J. Jeganathan, A. Ghrayeb, and L. Szczecinski. "Spatial modulation: optimal detection and performance analysis". In: *IEEE Communications Letters* 12.8 (Aug. 2008), pp. 545–547. ISSN: 1089-7798. DOI: [10.1109/LCOMM.2008.080739](https://doi.org/10.1109/LCOMM.2008.080739).
- [26] Jeyadeepan Jeganathan, Ali Ghrayeb, and Leszek Szczecinski. "Generalized space shift keying modulation for MIMO channels". In: *2008 IEEE 19th International Symposium on Personal, Indoor and Mobile Radio Communications (2008)*. DOI: [10.1109/pimrc.2008.4699782](https://doi.org/10.1109/pimrc.2008.4699782).
- [27] Jeyadeepan Jeganathan et al. "Space shift keying modulation for MIMO channels". In: *IEEE Transactions on Wireless Communications* 8.7 (2009), 3692–3703. DOI: [10.1109/twc.2009.080910](https://doi.org/10.1109/twc.2009.080910).
- [28] John G. Proakis and Masoud Salehi. *Digital Communications*. 5th ed. McGraw-Hill, 2008.

-
- [29] Y. Li and A. Nosratinia. "Grassmannian-Euclidean superposition for MIMO broadcast channels". In: *2012 IEEE International Symposium on Information Theory Proceedings*. July 2012, pp. 2491–2495. DOI: [10.1109/ISIT.2012.6283964](https://doi.org/10.1109/ISIT.2012.6283964).
- [30] Y. Li and A. Nosratinia. "Product Superposition for MIMO Broadcast Channels". In: *IEEE Transactions on Information Theory* 58.11 (Nov. 2012), pp. 6839–6852. ISSN: 0018-9448. DOI: [10.1109/TIT.2012.2209862](https://doi.org/10.1109/TIT.2012.2209862).
- [31] J. Ling et al. "Multiple transmit multiple receive (MTMR) capacity survey in Manhattan". In: *Electronics Letters* 37.16 (Aug. 2001), pp. 1041–1042. ISSN: 0013-5194. DOI: [10.1049/el:20010693](https://doi.org/10.1049/el:20010693).
- [32] Zhiqiang Liu, Yan Xin, and G. B. Giannakis. "Space-time-frequency coded OFDM over frequency-selective fading channels". In: *IEEE Transactions on Signal Processing* 50.10 (Oct. 2002), pp. 2465–2476. ISSN: 1053-587X. DOI: [10.1109/TSP.2002.803332](https://doi.org/10.1109/TSP.2002.803332).
- [33] Magnus R. Hestenes and Eduard Stiefel. "Methods of Conjugate Gradients for Solving Linear Systems". In: *Journal of Research of the National Bureau of Standards* 49.6 (Dec. 1952), pp. 409–436.
- [34] T. L. Marzetta and B.M. Hochwald. "Capacity of a Mobile Multiple-Antenna Communication Link in Rayleigh Flat Fading". In: *IEEE Trans. Info. Theory* 45.1 (Jan. 1999), pp. 139–157.
- [35] T. L. Marzetta and B.M. Hochwald. "Unitary space-time modulation multiple-antenna communications in Rayleigh flat fading". In: *IEEE Trans. Info. Theory* 46.2 (Mar. 2000), pp. 543–564.

- [36] M. L. McCloud, M. Brehler, and M. K. Varanasi. "Signal design and convolutional coding for noncoherent space-time communication on the block-Rayleigh-fading channel". In: *IEEE Transactions on Information Theory* 48.5 (May 2002), pp. 1186–1194. ISSN: 0018-9448. DOI: [10.1109/18.995648](https://doi.org/10.1109/18.995648).
- [37] R. Y. Mesleh et al. "Spatial Modulation". In: *IEEE Trans. on Vehicular Technology* 57.4 (2008), 2228—2241. DOI: [10.1109/tvt.2007.912136](https://doi.org/10.1109/tvt.2007.912136).
- [38] Petar Popovski et al. *Final report on the METIS 5G system concept and technology roadmap*. Apr. 30, 2015. URL: https://www.metis2020.com/wp-content/uploads/deliverables/METIS_D6.6_v1.pdf.
- [39] K. B. Petersen and M. S. Pedersen. *The Matrix Cookbook*. Version 20121115. Nov. 2012. URL: <http://www2.imm.dtu.dk/pubdb/p.php?3274>.
- [40] E. Polak. *Computational Methods in Optimization: A Unified Approach*. en. Google-Books-ID: YNaetHz0J4oC. Academic Press, May 1971. ISBN: 978-0-08-096091-3.
- [41] Chaitanya Rao and Babak Hassibi. "Analysis of Multiple-Antenna Wireless Links at Low SNR". In: *IEEE Trans. Info. Theory* 50.9 (Sept. 2004), pp. 2123–2130.
- [42] A. Scaglione et al. "Optimal designs for space-time linear precoders and decoders". In: *IEEE Transactions on Signal Processing* 50.5 (May 2002), pp. 1051–1064. ISSN: 1053-587X. DOI: [10.1109/78.995062](https://doi.org/10.1109/78.995062).

-
- [43] V. Tarokh and Il-Min Kim. “Existence and construction of non-coherent unitary space-time codes”. In: *IEEE Transactions on Information Theory* 48.12 (Dec. 2002), pp. 3112–3117. ISSN: 0018-9448. DOI: [10.1109/TIT.2002.805075](https://doi.org/10.1109/TIT.2002.805075).
- [44] V. Tarokh, N. Seshadri, and A. R. Calderbank. “Space-time codes for high data rate wireless communication: performance criterion and code construction”. In: *IEEE Transactions on Information Theory* 44.2 (Mar. 1998), pp. 744–765. ISSN: 0018-9448. DOI: [10.1109/18.661517](https://doi.org/10.1109/18.661517).
- [45] W. M. Boothby. *An Introduction to Differential Manifolds and Riemannian Geometry*. 2nd ed. San Diego, CA: Academic Press, 1986.
- [46] W. Zhao, G. Leus, and G. B. Giannakis. “Orthogonal design of unitary constellations for uncoded and trellis-coded noncoherent space-time systems”. In: *IEEE Trans. Info. Theory* 50.6 (June 2004), 1319—1327.
- [47] Y. Jing and B. Hassibi. “Unitary space-time modulation via Cayley transform”. In: *IEEE Trans. Signal Proc.* 51.11 (Nov. 2003), 2891—2904.
- [48] Lizhong Zheng and D. N. C. Tse. “Diversity and multiplexing: a fundamental tradeoff in multiple-antenna channels”. In: *IEEE Transactions on Information Theory* 49.5 (May 2003), pp. 1073–1096. ISSN: 0018-9448. DOI: [10.1109/TIT.2003.810646](https://doi.org/10.1109/TIT.2003.810646).
- [49] Lizhong Zheng and David N. C. Tse. “Communication on the Grassmann Manifold: A Geometric Approach to the Noncoherent Multiple-Antenna Channel”. In: *IEEE Trans. Info. Theory* 48.2 (Feb. 2002), pp. 359–383.